THEORETICAL ANALYSIS OF THE EFFECTS OF BUS OPERATIONS ON URBAN CORRIDORS AND NETWORKS

A Thesis
Presented to
The Academic Faculty

by

Felipe Castrillon

In Partial Fulfillment
of the Requirements for the Degree
Doctor of Philosophy in the
School of Civil and Environmental Engineering

Georgia Institute of Technology
December 2015

THEORETICAL ANALYSIS OF THE EFFECTS OF BUS OPERATIONS ON URBAN CORRIDORS AND NETWORKS

Approved by:

Professor Jorge Laval, Advisor
School of Civil and Environmental Engineering
Georgia Institute of Technology

Professor Kari Watkins
School of Civil and Environmental Engineering
Georgia Institute of Technology

Professor Randall Guensler
School of Civil and Environmental Engineering
Georgia Institute of Technology

Professor Bistra Dilkina
School of Computational Science and Engineering
Georgia Institute of Technology

Professor Michael Hunter
School of Civil and Environmental Engineering
Georgia Institute of Technology

Date Approved: 21 August 2015

ACKNOWLEDGEMENTS

My time at Georgia Tech has been an incredible journey made possible by many wonderful individuals. First and foremost, I want to thank Stephanie, my soon-to-be wife who has always supported and cared for me even when we were 1,083 miles away during the first few years. Being able share with you after long work days has kept me sane and in good spirit.

I am grateful for my advisor Jorge Laval for all of the hours of guidance and teaching. You have prepared me to think critically and creatively for any problem that I will face during my professional career. More importantly, you have been a friend that I can count on for many years to come. I look forward to reaching out when I need guidance or when I just want to catch up about life.

Another professor that has greatly shaped me at Georgia Tech is Randall Guensler, who was my co-advisor for many years. You were the first person who taught me how to do research and you have always been there for professional guidance.

Also, I want to thank the rest of my committee, Michael Hunter, Kari Watkins, and Bistra Dilkina for their guidance and comments. Having a committee with so many different perspectives has greatly improved my thinking and research approach during this dissertation.

To my friends in Atlanta, who have been a family away from home, I cannot thank you enough. Listing everyone will take longer than this document but I am particularly grateful to Ivan, Alejandro, Maria, Camilo, Tatiana, Renato, Carlos, Monica, Ciro and Barbara.

Finally, I want to thank my family, Andres, Lina, Nico, Adri and Juandi for always being close even when we were so far away. Your love and values makes me the person

that I am today and I do not have a lifetime to thank you enough. Furthermore, I want to acknowledge the continual support that I receive from my extended Castrillon and Londono family which has helped me greatly throughout these years.

TABLE OF CONTENTS

LIST OF TABLES

LIST OF FIGURES

SUMMARY

Bus systems have a large passenger capacity when compared to personal vehicles and thus have the potential to improve urban mobility. However, buses that operate in mixed vehicle traffic can undermine the effectiveness of the road system as they travel at lower speeds, take longer to accelerate, and stop frequently to board and alight passengers. Buses act as slow-moving bottlenecks that have the potential to create queue-spillbacks and thus increase the probability of gridlock. Currently, traditional metropolitan transportation planning models do not account for buses on roadway capacity. Also, research methods that study multimodal operations are often simulated or algorithmic which can only provide specific results for defined inputs.

The objective of this research is to model and understand the effects of bus operations (e.g., headway, number of stops, number of routes) on system performance (e.g. urban corridor and network vehicular capacity) using a parsimonious analytical approach with a few parameters. The models are built using the Macroscopic Fundamental Diagram (MFD) of traffic which provides aggregate measures of vehicle density and flow. Existing MFD theory, which accounts for corridors with only one vehicle class are extended to include network roadway systems and bus operations. The results indicate that buses have two major effects on corridors: the moving bottleneck and the bus short-block effect. Also, these corridor effects are expanded to urban networks through a vehicle density-weighted average. The models have the potential to transform urban multimodal operations and management as they provide a simple tool to capture aggregate performance of transportation systems.

CHAPTER I

INTRODUCTION

Urban congestion is high in the United States and Europe. According to the INRIX traffic scorecard, the average driver in America's ten worst traffic cities spent 47 hours in traffic during 2013 [1]. In the most congested European countries, this statistic was 58 hours in Belgium, 45 hours in Netherlands, 35 hours in Germany, and 35 hours in France. Congestion has historically been linked with economic growth. In the United States, after many years of steady or declining numbers during the economic recession, traffic congestion increased 6% in 2013. In the European continent there was an increase during the second, third and fourth quarters of 2013. This trend is especially strong in countries that showed positive economic growth. Congestion statistics for other countries are not available, but global trends indicate that urbanization increased from 49% to 53% during 2004 and 2013 (4). Also, large developing countries experienced a growth in vehicles per road kilometer from 2005 to 2011 in China (+145%), India (+18%, data available until 2009), Brazil (+19%) and Russia (+7.3%). These statistics suggest that global roadway demand is increasing.

In light of these trends, metropolitan areas need to find mobility solutions for current and growing traffic demands. However, approaches that have worked in the past, like expanding roadway capacity or building underground rail, may not be feasible due to economic, social and environmental hurdles. Construction of these systems is economically and environmentally expensive while implementation time is very long. Also, there is limited space or sometimes no space to build them in densely packed cities. Cheaper alternatives have become available with the adoption of Big Data

[1] Inrix: http://scorecard.inrix.com/scorecard/, url date: 2015-06-15

capabilities in the world of transportation. Cities can now detect traffic congestion from vehicle transponders, track transit fleets, capture individual trajectories from cellphones, and many other applications using Intelligent Transportation Systems (ITS). For a detailed summary on past, current, and near-future ITS capabilities please refer to Bin et al.(43). This new approach to alleviate congestion uses ITS to actively manage, control and optimize existing infrastructure resources at a lower cost than traditional methods. For instance, Tupper et al. (47) find that an ITS incident management strategy provides fuel savings over 30 times larger than other cost-saving strategies focused on the construction phase compared over an 8-year repaving schedule.

Managing bus systems can be an essential part of this new approach. For example,El-Geneidy et al. (20) demonstrate how Automatic Vehicle Location (AVL) and Automatic Passenger Counters (APC) can be used to improve mean travel times and service reliability on a bus line. Also, a study by Watkins et al. (48) finds that providing real time transit information for users reduces perceived and actual waiting times for passengers. Such improvements make bus operations more attractive to users. This can provide many benefits to urban roadway mobility as buses have a large passenger capacity when compared to personal vehicles. Therefore, a switch from car users to buses has the potential to decrease the number of vehicles on the road which can lead to congestion reduction. Also, from the operation side, bus systems are very flexible to modify as fleet sizes, frequencies, stops, and routes can be changed rapidly at a low cost.

Bus operations also create negative effects when sharing the road with personal vehicles. They can undermine the effectiveness of the road system for everyone, as they drive at lower speeds, take longer to accelerate, and stop frequently to board and alight passengers. In traffic flow, buses are known as moving bottlenecks that have the potential to create queue-spillbacks thus increasing the probability of gridlock.

In order to understand the full impact of buses in an urban setting, the effect of bus operations on traffic flow must be quantified.

Various research methods have studied the reduction of vehicle capacity from bus operations. These methods are either simulated (42; 32; 50; 51; 54; 49; 27), algorithmic (5), analytical (19) or a combination (49). Simulation and algorithmic approaches are laborious to build and can take significant time to run, especially if the system is large. Also, they do not provide general insight into how input parameters (bus operation parameters, signal timing, block length) affect the output capacity of a system. Existing analytical models are more attractive as they can provide general insight into the problem and help to develop the models in this work.

Current practice does not consider these effects. Transportation planning agencies in the United States rely on forecasting models such as the four-step model or activity based models (37). These models load vehicles into the roadway system through traffic assignment methods which do not consider bus operations. Only by adjusting calibration constants in the validation process can real-life traffic conditions be captured (1). However, this "black-box" approach does not provide any insight into the bus effects on capacity. Transportation agencies often employ micro-simulation corridor studies with commercial software packages that can account for bus operations (46). However, simulation can only give specific results for a particular set of inputs and generalizations are difficult to make. Also, as the simulated area grows, the computational costs and the data collection efforts increase very rapidly.

In order to measure urban traffic conditions, the Macroscopic Fundamental Diagram (MFD) is a useful tool that gives the average flow on a network as a function of the accumulation of vehicles inside the network (13). This relationship is invariant to traffic demand changes across days and time of days. However, it is dependent on network topology and control parameters such as block length, existence of turn-only lanes, and traffic signal settings.

Methods exist to estimate the MFD analytically for simple homogeneous roadway corridors(15) and for stochastic roadway corridors where parameters vary across time and distance (33), with the assumption that traffic is evenly distributed along the corridor. This constitutes the starting point for this dissertation.

1.1 Research objectives

The research objective of this dissertation is to test the hypotheses that the Macroscopic Fundamental Diagram (MFD) can be used to capture the impacts of buses in congested urban corridors and networks. In particular, if MFD theory can be extended to account for the main cause-and-effect mechanisms between the operational characteristics of buses (e.g., frequency, number of stops, number of routes) and system performance (e.g. network capacity, mean travel times). Notice that existing MFD theory focuses on corridors, and must be extended for networks.

1.1.1 Scope

The scope of the dissertation focuses on the vehicle throughput of mixed traffic operations. It does not include possible changes in the mode split (i.e., changes in car-bus market share) or departure time choice due to changes in bus operations.

1.2 Overview

The major component of the dissertation is the analytical models. For validation purposes, model outputs are compared against synthetic data from a micro-simulation model especially built for this purpose. Since both the theory and the simulation methods are based on the kinematic wave model and use the same input parameters, the simulation model is the ideal tool for comparison. Note that microscopic simulation is straightforward to build, but difficult to derive any meaningful insight from it. In contrast, the model is macroscopic and analytical.

The dissertation is divided into three main parts each one dealing with a different

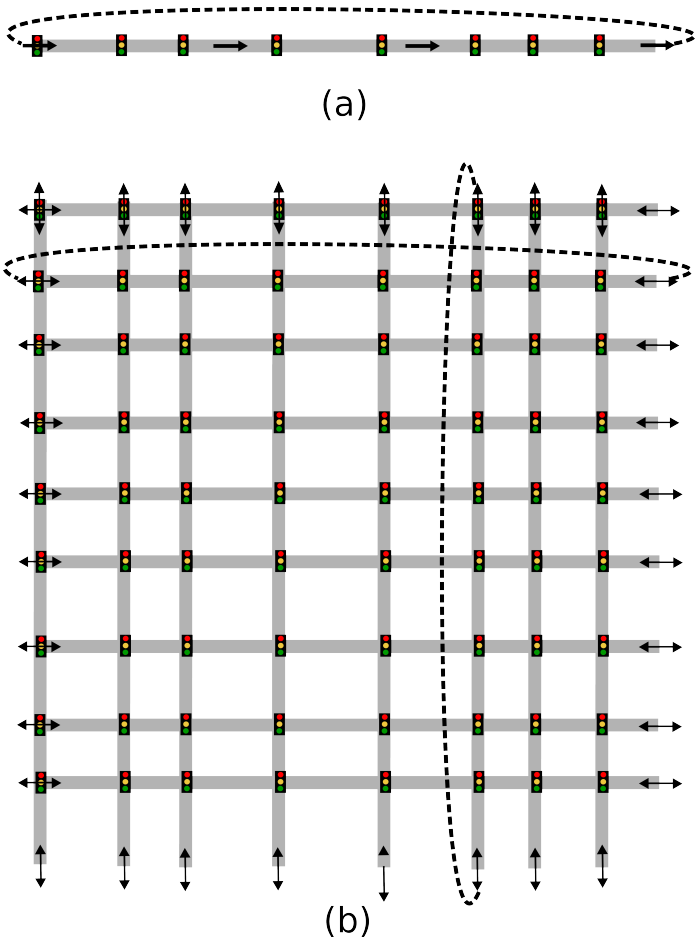

Figure 1: (a) ring corridor, and (b) ring network

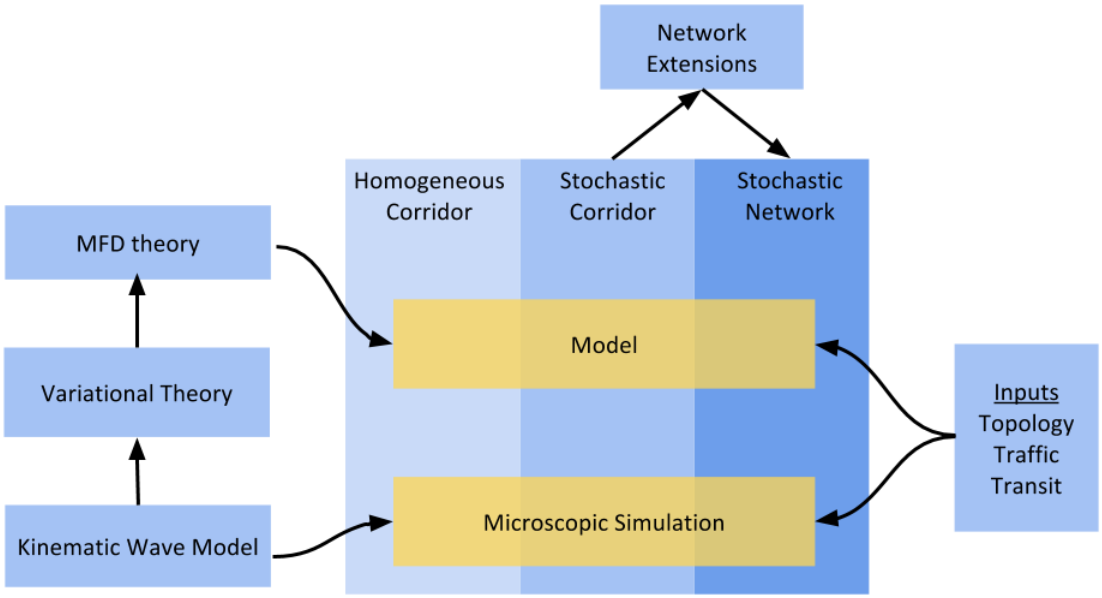

Figure 2: Dissertation road map

roadway system. The first part focuses on homogeneous ring-corridors, which have constant signal parameters and street segment lengths. Fig. 1(a) shows an example of a ring-corridor. In this section, the analytical method to solve homogeneous corridors, called the "method of cuts", is extended to account for bus operations. These systems are very simplistic compared to real-world corridors, but starting with an uncomplicated case provides important insight for the next sections. The second part deals with stochastic corridors, where signal parameters and segment lengths vary according to a defined distribution. Existing models for stochastic corridors (33) are extended to develop the models. This type of corridor is more realistic but still does not consider any turns or routing. The last part considers network corridors, which are Manhattan-grid systems comprised of stochastic corridors; ; see fig. 1(b). The corridor models are extended to account for network operations and bus systems. Final conclusions and future work is discussed on the last chapter.

CHAPTER II

BACKGROUND

This section provides a survey of the existing literature on multimodal modeling, the MFD, and moving bottleneck theory.

2.1 Multimodal modeling

The effect of bus operations on vehicular flow has been studied using simulated methods. The limitations of these studies is that they can only provide specific outputs given some input parameters.

Geroliminis et al. (27) studied the shape of a 3-D bi-modal MFD relating vehicle flow and the accumulation of cars and buses from a simulation of the San Francisco downtown. The study finds a well-defined MFD that is monotonically increasing as either the accumulation of cars and buses increase.

Ngan et al. (42) studied the effectiveness of Transit Signal Priority (TSP) and other traffic and transit parameters using simulation. Koshy & Arasan (32) analyzed the effects of bus stops on average speeds using a simulated environment. Zhao et al.(50; 51) employed a cellular automaton model to analyze the interaction between bus stop placement and nearby signals. Zhu (54) used a cellular automaton model to study bus and car performance on dedicated lanes and mixed traffic.

Algorithmic methods use variational theory to provide results that are usually computationally faster than simulation methods. However, like simulation, results are specific to defined inputs. Boyaci & Geroliminis (5) simulated bus trajectories as bottleneck links throughout the variational theory time-space graph network. The MFD cuts are obtained by simulating observer paths throughout the time-space graphs and estimating average speeds and maximum passing rates for each. The study does not

consider the moving bottleneck effect of slow-moving bus vehicles. Xie et al. (49) simulated bus trajectories as straight line paths traveling at the average bus speed. The method reduces link costs of nearby links to the bus trajectory by the percentage of lanes that the bus is not blocking $(n-1)/n$.

Existing analytical methods are preferable to simulated and algorithmic method as they provide general insight. Eichler (19) studied the moving bottleneck effect on Bus Lanes with Intermittent Priority (BLIP) operations. Xie (49) incorporated the moving bottleneck effect as an upper boundary cut to the MFD without buses. The methods are a great starting point for the project, but have a few areas of improvement. First, the capacity reduction from the bus-signal interactions is not considered; more on this effect later. Secondly, the average bus speed is usually not known as traffic conditions affect operating speeds. Finally, the moving bottleneck effect has not been formulated with respect to MFD theory.

Other applicable studies focus on optimizing the space allocation between different modes (53) and the morning commute problem with mode choice (30).

2.2 Urban macroscopic modeling

In order to aggregate varying traffic states arising from urban operations, a macroscopic approach is necessary. Macroscopic traffic relationships have been proposed in the past (28; 3) but are limited to light traffic conditions. Only recently has there been a strong interest on macroscopic modeling after Daganzo (13) proposed the Macroscopic Fundamental Diagram (MFD). The idea is that the average flow on a network is mostly a function of the accumulation of vehicles inside the network, invariant of the demand across days and time of days. The MFD shape is dependent on network topology and control parameters such as block length, existence of turn-only lanes, and traffic signal settings.

For real-life cities, network properties and congestion levels vary across different

areas which violates MFD conditions. To address this, Daganzo proposes dividing large areas into neighborhoods, called reservoirs, with similar traffic properties. Using feedback monitoring and control policies, such as signal timing, cordon pricing,or lane utilization by mode, densities can be controlled on each neighborhood in order to avoid congested conditions. Research in this area focuses on neighborhood portioning(31) and boundary control policies (2). This approach can overcome some of the shortcomings from existing travel demand models, which require a large number of inputs to populate O-D tables, and its results are hyper-sensitive to inputs which leads to high inaccuracies(9; 52).

The existence of the MFD has been verified in simulated environments (29; 25; 6), and empirically (26). Recent MFD research has focused on the effect of traffic inhomogeneity across a network (24; 36), issues dealing with bifurcation and instability (14; 6), and the effect of turns and routing (22).

Methods exist to estimate the MFD analytically for simple arterial corridors with uniform block lengths and signal parameters (15) and for stochastic corridors where parameters vary across time and distance (33). Both theories assume no-turns and a homogeneous distribution of traffic along the corridor. The theories constitute the starting point for the proposed research. MFD theory is built upon the kinematic wave (KW) traffic model (35; 44) and the variational theory (VT) (10; 11) formulation to solve the KW model. These are described first before going into the MFD formulation.

2.3 Kinematic wave model

The kinematic wave (KW) model (35; 44) is a scalar conservation law for the local density of vehicles on a road at time t and location x, supplemented with a fundamental diagram (FD) that gives the flow $q(k, t, x)$, as a function of the local density $k(t, x)$. For a road without entrances or exists, the conservation law is:

$$\frac{\delta k}{\delta t} + \frac{\delta q(k)}{\delta t} = 0, \tag{1}$$

where q is the flow and k is the density of the system. A shockwave between two traffic states in the fundamental diagram is given by the speed:

$$s = \frac{\delta q(k)}{\delta k} \tag{2}$$

The system described by eq. 1 belongs to the family of first order nonlinear hyperbolic partial differential equations (PDEs). In this study, a triangular fundamental diagram is assumed which indicates that acceleration shock waves travel at nearly constant speeds which is consistent with empirical data (7; 8; 38).

The triangular fundamental diagram can be described by two traffic regions separated by a capacity state as shown in fig. 3(a). For low densities, the free-flow branch has a slope equal to the free-flow speed $w^\sharp$. Notice that in this region, the flow of vehicles increases as the density increases. Also, as densities increase on the free-flow branch, an optimal density is reached at the flow capacity Q. At this point, no more vehicles can be introduced into the road without decreasing the flow. For densities that are higher than the capacity state, a congestion branch is given with a slope equal to the congested wave speed $-w^\flat$. In this region the flow decreases as density increases. Notice in the figure that the speed of a shock wave between two traffic states S and A can be obtained by drawing a straight line on the FD between the two states and finding the slope s.

2.3.1 Kinematic wave-moving bottleneck (KW-MB) theory for freeways

The moving bottleneck model was first reported in Gazis and Herman (23), but it was Newell (41) who puts it in the context of kinematic wave (KW) theory. The theory is particularly useful when the fundamental diagram (FD) on the roadway is assumed to be triangular in shape. The empirical validation of the MB model can be found in (38), while numerical methods for incorporation into simulation models are presented in (16).

A moving bottleneck creates a free-flow traffic state downstream of its trajectory

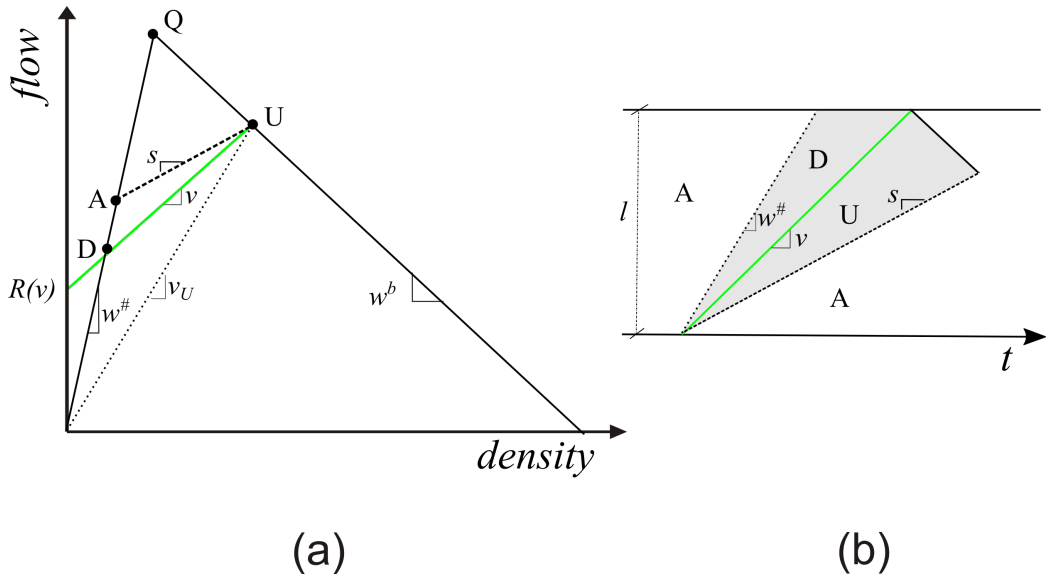

Figure 3: Moving bottleneck effect. (a) Fundamental diagram with moving bottleneck "cut". (b) Time-space diagram showing the effects of a moving bottleneck trajectory on upstream and downstream traffic states

denoted by D and a congested traffic state upstream given by U. These traffic states are plotted on the fundamental diagram in fig. 3(a). The downstream flow can be obtained by the capacity of the bottleneck $Q(n-1)/n$ where n is the number of lanes. Also, the bus is introduced in the FD as a KW traffic shock wave between the two traffic states D and U having speed v. This shock wave creates an upper bound flow to the fundamental diagram as vehicles cannot pass the bus on one of the lanes.

An example of the moving bottleneck effect on a street segment with length l can be observed on the time-space diagram in fig. 3(b). Here, a traffic state A is present before and after the bus travels through the segment. Notice, how the bus creates traffic states D and U and how the FD is used to build the traffic shock waves between all of the observed traffic states A, D and U. For instance, the shock wave speed between A and U is given by s.

2.4 Variational theory

Solving the KW model through time-space diagrams is a cumbersome task as all traffic shock waves need to be considered. This is where the variational theory (VT) formulation (10; 11) becomes useful, which is a simple and exact solution to the kinematic wave (KW) model. The FD is defined as a Hamilton-Jacobi partial differential equation:

$$\begin{aligned} \frac{\delta N}{\delta t} &= Q(-\frac{\delta N(t,x)}{dx}, t, x) \\ N(B) &= N(G) \end{aligned} \tag{3}$$

Where $N(t,x)$ is the cumulative count of vehicles at a location x by time t, with $\delta N/\delta t$ as the flow and $\delta N/\delta x$ as the density. An example of a cumulative count curve is shown on fig. 4 where every step represents an increase in vehicle count. Notice that $N(t,x)$ is an increasing function in time.

The VT formulation is solved using the the Hopf-Lax formula (34; 17). The solution gives the number of vehicles N that have crossed location x by time t:

$$N(P) = \underset{B\epsilon\beta_P}{inf}\{N(B) + \Delta_{BP}\}, \tag{4}$$

where, $P = (x_P, t_P)$ is the time-distance coordinate of a generic point, β_P is the known boundary in the domain of dependence of P, and Δ_{BP} is the maximum number of vehicles that can cross the minimum path connecting boundary point $B = (t_B, x_B)$ and point P. Notice that in the absence of bottlenecks like red signals or buses, straight line paths from B to P provide minimum paths. Fig. 4(b) shows a visual representation of the solution.

Variational theory problems can be solved by building graph networks as in fig. 4(c) and applying shortest path algorithms. A triangular fundamental diagram is assumed with free-flow speed $\omega^{\#}$, congested wave speed $\omega^{\flat}$, maximum flow $Q = \omega^{\#}\omega^{\flat}/(\omega^{\#} + \omega^{\flat})$ and jam density $\kappa = Q(1/\omega^{\#} + 1/\omega^{\flat})$. The first step is to define the known boundary β and to determine discrete boundary points. Then, red signals are

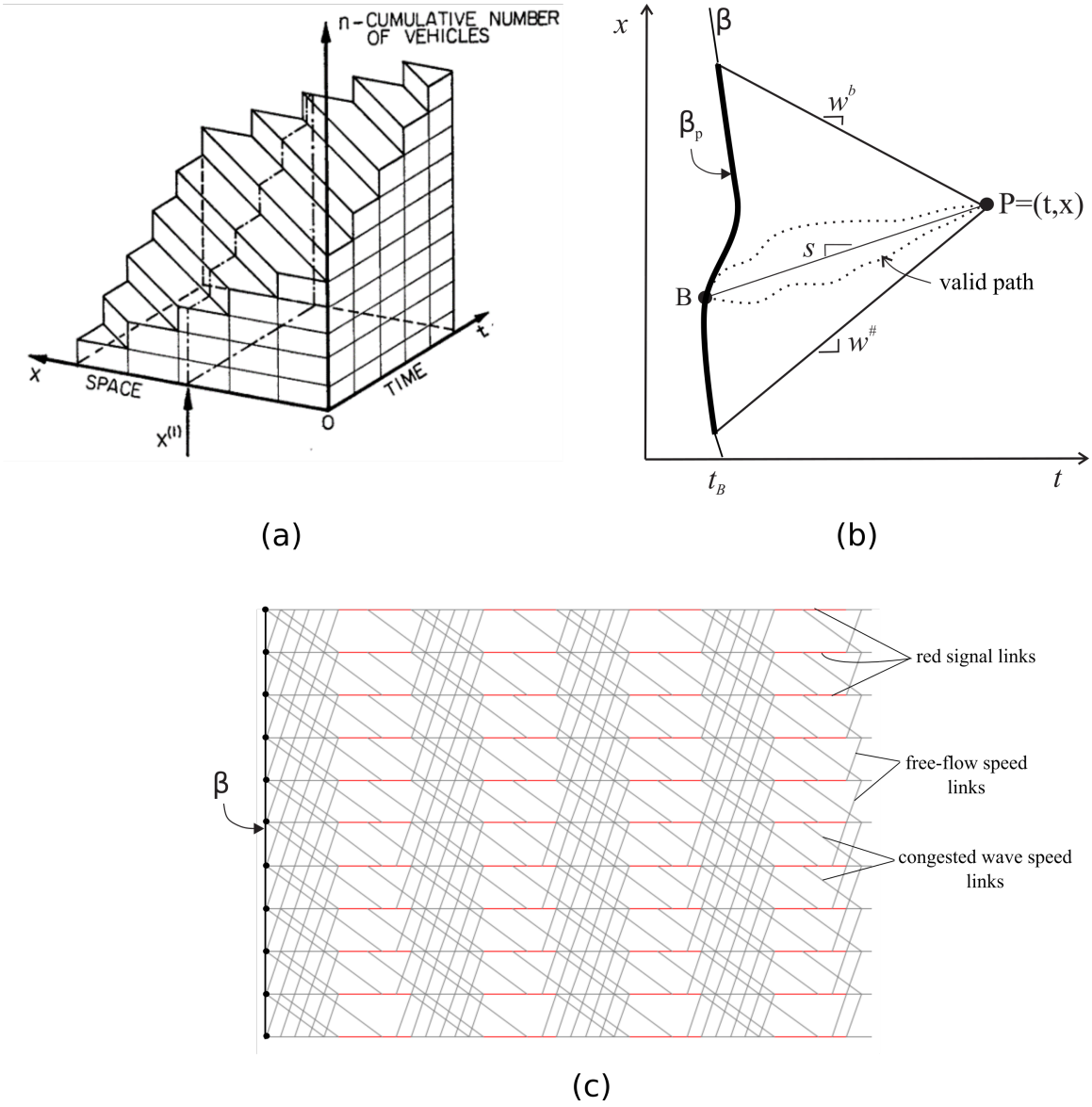

Figure 4: (a) Cumulative count curve across time and space, (b) visual representation of a variational theory problem, (c) variational theory network graph for the time-space diagram of a corridor

inserted as short-cut links with nodes at the beginning and end of the signal. For the graph to be validly connected, each boundary node and signal node is aligned with inbound and outbound links having speeds $\omega^{\#}$ and $\omega^{\flat}$. Then, nodes are placed wherever links cross. Notice that links can be stopped when encountering a short-cut link as shown on the figure.

Link weights are defined by the maximum number of vehicles that can cross a given link. This can be estimated by the maximum passing rate multiplied by the time elapsed on the link. The maximum passing rate of red signals is zero since no vehicles can cross them. For free-flow speed links, the maximum passing rate is also zero since no cars can go faster than this speed. Finally, the passing rate of congested links is $\kappa\omega^{\flat}$. The cumulative count N can now be solved by defining a point P in the time-space diagram and solving shortest path problems from the boundary points to this point.

For more information on partial differential equations and Hamilton-Jacobi equations please refer to Evans (21)

2.5 MFD Theory

In order to estimate the MFD, consider an initial value VT problem applied to the time-space diagram of a corridor; see figure 5(a). The boundary $N(0,x)$ is given by an uniform density k. Without any loss of generality, the location origin is set at $x_P = x_0 = 0$ and the initial vehicle count at $N(0,0) = N_0$. This gives the vehicle count at the boundary as $N_0 + xk$ where x is the location along the corridor. To obtain the flow, the vehicle count difference at x_0 is divided by the time window:

$$\begin{aligned} \frac{N(P) - N_0}{t} &= \inf_{B \epsilon \beta_P} \{N_0 + xk + \Delta_{BP}\}/t - N_0/t \\ q &= \inf_{w} \{wk + R(w)\}. \end{aligned} \tag{5}$$

Where w is the average speed of the path, Δ_{BP} is the maximum number of vehicles that can pass the minimum path and $R(w) = \Delta_{BP}/t$ is the maximum passing rate.

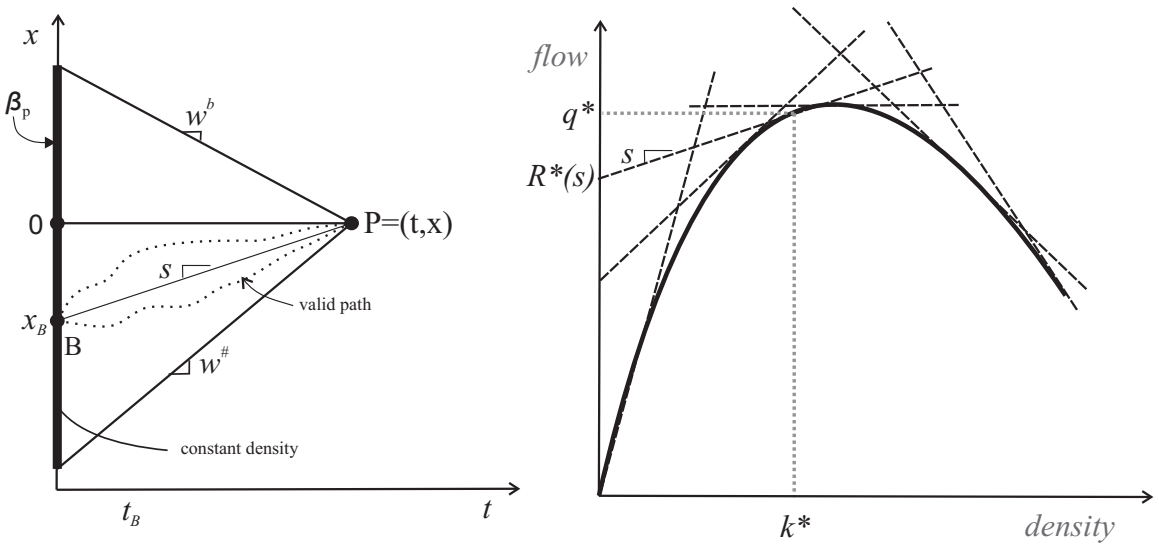

Figure 5: (a) Initial value variational theory problem with constant density on the boundary. For each boundary point B, the minimum path is obtained from all valid paths. (b) Each minimum path corresponds to a upper boundary cut to the MFD

The solution for the MFD is the lower envelope of the family of "cuts" $wk + R(w)$. Notice in 5(b) how upper boundary "cuts" are built from the set of minimum paths.

2.5.1 "Method of cuts" for homogeneous corridors

Homogeneous corridors have deterministic parameters for green times g, red times r, offsets o and street segment lengths l. The offset is defined as the cycle time difference between two intersections.

Daganzo and Geroliminis (15) demonstrated an approximation method to calculate the MFD for homogeneous corridors. First, consider the time-space diagram on fig. 6(a) and notice the minimum paths emanating from the $t = 0$ boundary and reaching point P. It is easy to see that minimum paths follow repeated patterns throughout the network due to the homogeneity conditions of the corridors. Notice that the figure only shows the minimum paths that begin at signalized intersections, but in reality, the number of boundary points are infinite.

In order to overcome this limitation, an approximation method is used where only a few of the minimum paths are considered. These paths are periodic in nature as

they repeat across the time-space diagram. This means that only one period or cycle of the pattern needs to be accounted for, as shown on the free-flow paths on 6(b) and congested wave paths on 6(c).

The first free-flow path begins at "start", travels with speed $w^{\#}$, stops at the first red signal encountered at intersection I_{max} and waits until the end of the red signal. Subsequent paths also begin at "start", and travel with speed $w^{\#}$, but stop prematurely during the green phase at intersections $i, 0 \leq i < I_{max}$, and then wait until the end of the next red signal. Congested paths are built in a similar fashion, but use speed w^{β}. For each of these paths, an average velocity and a maximum passing rate are evaluated analytically in order to build the "cut" from eq. 5. The maximum intersection is given:

$$I_{max} = 1 + max\left\{i\colon i(l/v - o)/c - \lfloor i\colon i(l/v - o)/c \rfloor \leq g/c\right\} \tag{6}$$

Where, l is the block length, o is the offset between two intersections, g is the green phase duration, and c is the cycle time.

The average speed for a cut that stops at intersection i is:

$$w = \frac{li}{li/u + G + R} \tag{7}$$

where G is the left-over green time and R is the left-over red time when the vehicle stops at the intersection. For the fastest cut, which stops at I_{max}, these values are estimated as $G = 0$ and $R = I_{max}(l/u - o) - g$. For the other cuts, $G = i(l/u - o)$ and $R = r$, where r is the red phase duration.

For the free-flow wave cuts, the passing rate is given by GQ and for the congested wave cuts it is $l\kappa + GQ$.

2.5.2 Renewal reward theory

Before the stochastic corridor model is presented, a brief summary of renewal rewards theory is given. This theory is used to solve the model and is also used to solve other quantities throughout the dissertation.

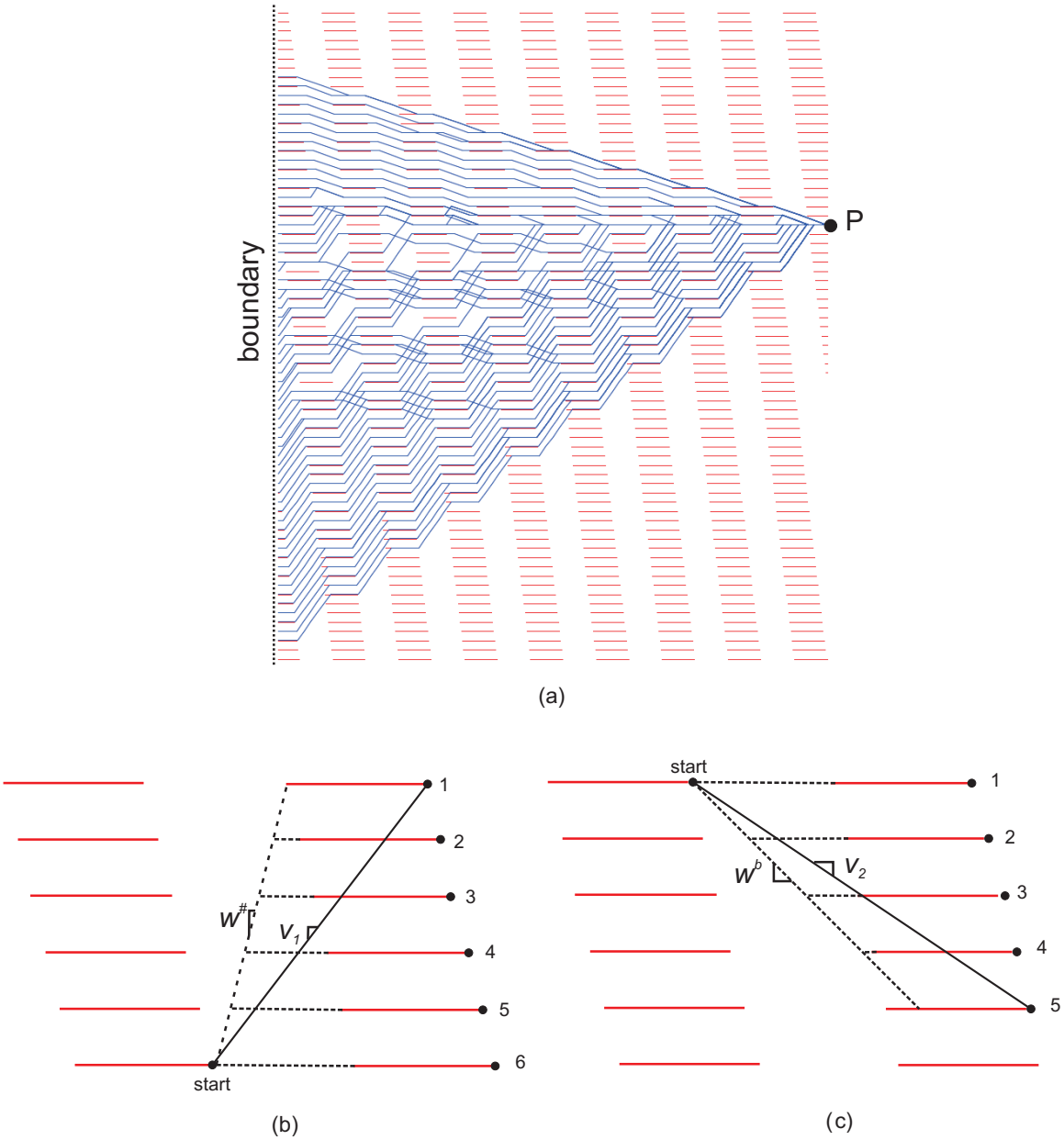

Figure 6: (a) Variational theory problem for a homogeneous corridor. Minimum paths from the boundary to point P are shown in blue. (b) Paths to build free-flow cuts. (c) Paths to build congested cuts.

A renewal process is a counting process $N(t)$,$t \geq 0$ where interarrival times T_i, $i \geq i$, between events n_{i-1} and n_i are independent and identically distributed (45). An transportation engineering example of a renewal process is the number of buses that have arrived at a bus stop by time t where bus headways are i.i.d.

A renewal rewards process is an extension of a renewal process where each time a renewal occurs, a reward R_i, $i \geq 1$, is received. The reward is i.i.d. but can depend on the length of T_i. The total reward received by time t is obtained by:

$$R(t) = \sum_{i=1}^{N(t)} R_i \tag{8}$$

The expected average reward is given by:

$$R(t) = \lim_{t \to \infty} = \frac{E[R]}{E[T]} \tag{9}$$

Renewal rewards theory is used extensively throughout the paper since variational theory paths have repeating patterns throughout the time-space vt graph where each pattern can be expressed as a renewal occurrence or "cycles".

2.5.3 Stochastic corridor model

Stochastic corridors have varying segment lengths, green times, and red times across time and space defined by random variables l, g, r respectively. The variables follow a normal distribution with mean $\mu_{\_}$, standard deviation $\sigma_{\_}$ and coefficient of variation (cov) $\delta = \mu_{\_}/\sigma_{\_}$, where $\_$ is a placeholder for the random variables. Vehicles on the corridor follow a triangular fundamental diagram as defined by the KW theory of traffic.

For stochastic corridors, obtaining all valid paths is a cumbersome task because paths do not follow periodic patterns across the network. Laval & Castrillon present an approximation method that only requires five independent paths (33). Each path is built by a different routing strategy s throughout the variational theory time-space graph network starting at P and traveling backwards in time until reaching β_P. The

strategies are described below where ω represents the wave speed and can take either the free-flow speed $\omega^{\#}$ or the congestion wave speed ω^{β}:

- s_0: stay in the same intersection
- s_1^{ω}: travel at speed $-\omega$, stop when hitting a red phase and wait until the beginning of the red phase to continue the trajectory with speed $-\omega$
- s_2^{ω}: travel at speed $-\omega$, stop at every intersection and wait until the beginning of the next red phase to continue the trajectory with speed $-\omega$

The MFD "cut" for each strategy s is solved by a renewal reward process where each renewal cycle starts at the beginning of a red signal, travels backward in time with the described behavior and ends at the subsequent beginning of a red signal. This behavior continues until the boundary β_p is reached. For a renewal rewards process, the time elapsed and the reward is necessary for each cycle. The time elapsed is straightforward and is given by a T random variable. The reward is defined as the contribution to the vehicle count given by random variable N, which is obtained from $Lk + \Delta$ where L is the distance covered by the cycle and Δ is the maximum number of vehicles that can cross the path. Renewal rewards theory gives the distribution of a cut s as a normal random variable with mean μ_s and variance σ_s^2/t, where:

$$\begin{aligned} \mu_s &= \mu_N/\mu_T \\ \sigma_s &= \frac{\mu_N^2}{\mu_T}\left(\delta_N^2 + \delta_T^2 - 2cor(N,T)\delta_T\delta_N\right) \end{aligned} \tag{10}$$

Recall that the MFD is given by the minimum envelope of all cuts as defined on 5. Therefore, for each density value k the minimum of the five cuts is estimated. The cumulative density function (CDF) of the the flow $q(k)$ is approximated as the probability that q is smaller than the five cuts:

$$F_{q(k)}(q) = 1 - (1 - F_{s_0}(q))^B \prod_{s\epsilon\Omega}(1 - F_{s,k}(q)), \tag{11}$$

where $F_{q(k)}(q)$ is the distribution of the flow with density k and Ω is the set of the five strategies. Notice that the "standing observer" strategy given by s_0 is replicated for each of the B blocks, giving us B "cuts".

2.5.4 Canonical formulation

The formulation is simplified in order to reduce the number of parameters. The mean and cov values in eq. 10 are formulated using the dimensionless length λ, the red/green ratio ρ, and the coefficient of variation δ. These random variables are used extensively throughout the rest of the dissertation since they are the only three inputs needed to construct a corridor or a network realization. The variables are defined:

$$\lambda = l/l_c, \;\; l_c = \frac{\mu_g}{1/w + 1/u}, \tag{12a}$$

$$\rho = \mu_r/\mu_g, \tag{12b}$$

$$\delta = \delta_l = \delta_g = \delta_r. \tag{12c}$$

The maximum flow and jam density are normalized to 1, which re-scales the triangular fundamental diagram parameters in units of critical headway and units of jam density:

$$Q = 1, \kappa = 1, \tag{13a}$$

$$\omega^\sharp = \theta + 1, \tag{13b}$$

$$\omega^\flat = 1/\theta + 1, \tag{13c}$$

where $\theta = w^\#/w^\flat$. Finally the MFD exhibits a "symmetric property" with respect to a line that crosses the maximum capacity point and the point $(0, \kappa/2)$. A density transformation is performed to make the MFD symmetric:

$$k' = k - \frac{1}{2}\left(1 - \left(\frac{1}{\omega^\flat} - \frac{1}{\omega^\sharp}\right) q\right). \tag{14}$$

Notice that the transformed density is now applied to eq. 11. The canonical formulation for the mean and cov of each "cut" is omitted here, but can be readily found

in the reference (33).

2.5.5 Short-block effect

The short-block effect, described on Laval and Castrillon (33), occurs when intersections are close to each other and the capacity of an intersection is reduced by nearby intersections. The condition for short blocks is given as $\lambda < 1 + \delta$.Fig. 7(a) shows how VT minimum paths are altered when short-blocks are present. This behavior becomes even more complex as the number of blocks grows since the paths can jump from intersection to intersection in an unpredictable manner; see Fig. 7(b). The consequence of the short-block effect is that the capacity cut from strategy s_0 does not provide a tight upper bound. Therefore a regression equation is employed to capture at tighter capacity "cut":

$$\frac{1}{1 + \rho(0.58\delta\lambda + 1.64\lambda^2 - 5.3\lambda + 4.99)}. \tag{15}$$

Notice, on Fig. 7(c) that bus trajectories also create a short-block effect. When buses cross the influence triangle, then the shortest path is altered. This creates very complex behavior as shortest path jumps from intersection to intersection often taking the bus trajectory for several blocks; see Fig. 7(d).

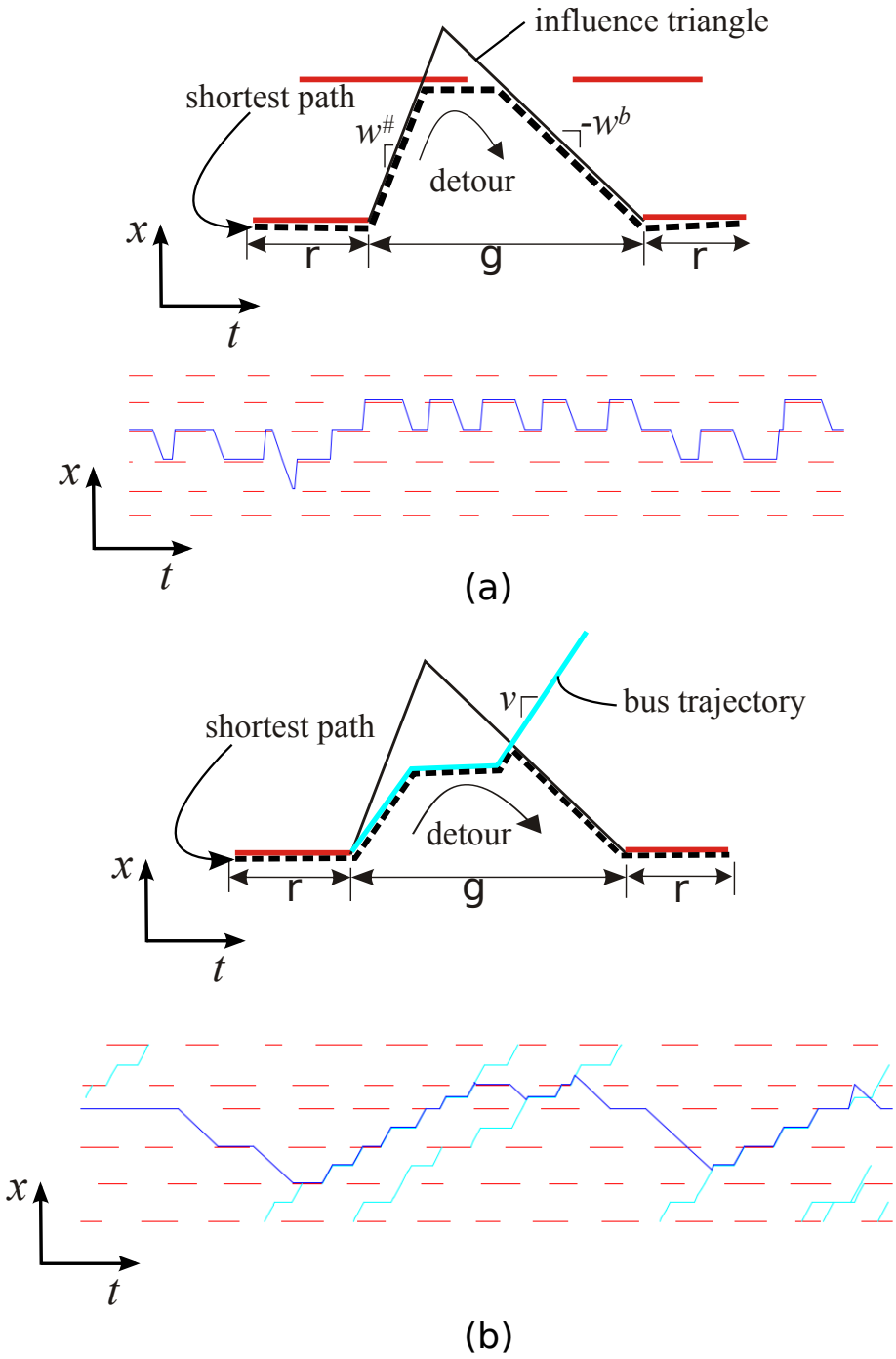

Figure 7: (a) Minimum paths are altered by short-blocks. (b) Minimum path simulation starting and ending in the same intersection. (c) Buses alter minimum paths similar to short-blocks. (d) Minimum path simulation with bus trajectories.

CHAPTER III

SIMULATION

This chapter deals with the development of the simulation software which is used to solve the KW model and to help guide analytical results on subsequent chapters.

3.1 Link simulation model

A deterministic version of the famous NaSch CA model (39) is used which gives the exact solution to the kinematic wave model with a triangular fundamental diagram as demonstrated by Daganzo (12). Time and space are discretized by Δt and Δx, where each vehicle occupies one cell. A variable with a dimensionless quantity is described with a "hat", e.g. $\hat{x} = x/\Delta x$. For a single link, the dimensionless position is given by:

$$\hat{x}(n, \hat{t}+1) = min\{\hat{x}(n, \hat{t}) + w^{\sharp}/w^{\flat}, \hat{x}(n-1, \hat{t}) - 1\} \tag{16}$$

Where $\hat{x}$ is the dimensionless position measured in units of the Δx, n is the vehicle number, $\hat{t}$ is dimensionless time measured in units of Δt, and $w^{\sharp}/w^{\flat}$ is an integer.

The advantage of this formulation over commercial simulation packages is that it solves the KW model with a fast execution time appropriate for large networks. Also, it gives flexibility in controlling inputs and operational rules (car-following, lane changing, bus operations). Lastly, the model requires only a few inputs and helps to isolate the effect of bus operations and reduce the number of confounding factors.

3.2 Urban simulation model

The network simulation package extends the link simulation model to include traffic intersections, turns, routing and lane-changing. A beta version of the software can

be accessed online [1]. The simulation software has user-friendly controls, a real-time visualization component to see how vehicles interact in the system, and an MFD output component; see fig. 8.

The simulation tool is adapted from an existing Java-based simulation which is a one-lane, unidirectional, square grid network [2]. The modified software tool developed in this project adds the following features:

- Corridor vs. network
- One direction, two directions (E-W,W-E) or four directions (N-S,S-N,E-W, W-E)
- Number of lanes
- Lane changing rules
- Bus vehicle class
- Routing
- Modified GUI for user-friendly controls

Cars travel at free-flow speed 4 cells/time unit which corresponds to 80 km/hr when $\Delta x = 6.67$ and $\Delta t = 1.2sec.$. These parameters are similar to the range of values used in the field. Flow and density averages for a time aggregation period τ and a lane-distance aggregation area X are calculated by using Edie's generalized definitions (18):

$$q = \frac{D}{\tau X} \tag{17a}$$

$$k = \frac{T}{\tau X}, \tag{17b}$$

[1] MFD multimodal simulation: http://felipecastrillon.github.io/mfd_ simulation_ bus/

[2] MFD on unidirectional grid networks: http://trafficlab.ce.gatech.edu/node/1961

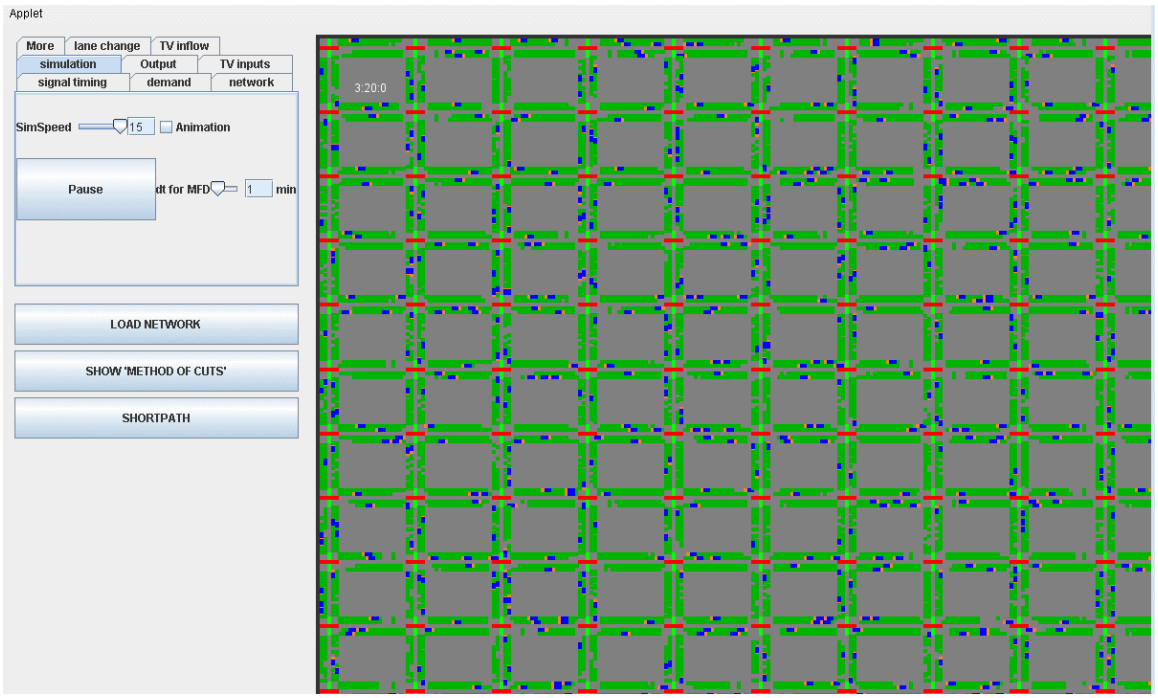

Figure 8: Simulation software

where q is the flow, k is the density, D is the sum of the distance covered by all vehicles, and τ is the sum of the time spent by all vehicles on the system. Output results are normalized whereas maximum flow is $Q = 1$ and jam density $\kappa = 1$.

Simple velocity based lane-changing rules are adapted from (40). The rules consist on determining whether there is an incentive to change lanes, and then looking for sufficient gap on the target lane before making the change. The incentive to change lanes has one important parameter called the "look ahead" value, which is the number of cells in front to look for another vehicle. If there happens to be a vehicle within the look ahead value, then the velocity of the vehicle ahead is compared to its own velocity. If the velocity is slower than its own, then the incentive to change lanes becomes active and it looks for a large enough empty gap on the target lane to make the change. The "look ahead" value used is 6 cells and the lane changing gap is 5 cells where a vehicle looks at 4 cells behind and 1 lane in front of the current cell location.

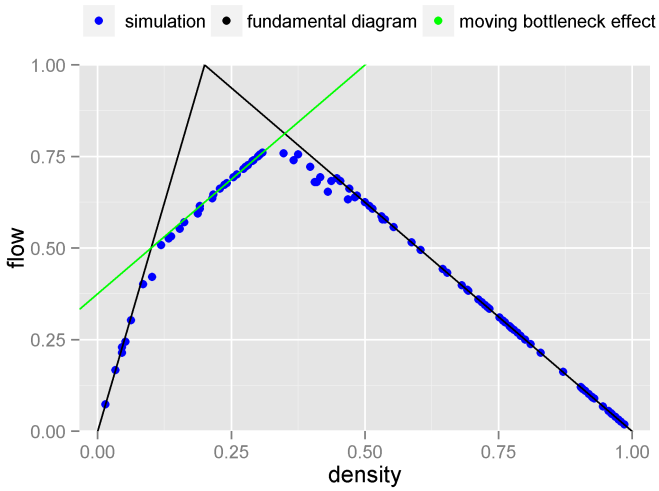

Figure 9: Comparison of a 2 lane ring corridor without traffic signals and with bus operations to the KW-MB model

The lane-changing rules are implemented to ensure that there is no loss of vehicular flow as predicted from the single-pipe kinematic wave model. As a demonstration, an experiment is performed where the simulation results of an unsignalized ring-corridor with 2 lanes and buses matches very well with the KW-MB model described earlier in fig. 9. The results indicates that the lane-changing rules do not reduce the predicted KW vehicle flow of the link with buses.

The simulation does not consider left-turn operations where vehicles look for sufficient turning gaps. Instead, vehicles ignore incoming traffic from the opposite direction to make turns. This is an unrealistic assumption, but it helps to isolates the moving bottleneck effect from confounding factors created from turning effects. This assumption needs to be studied further in the context of MFD theory but is outside of the scope of this research.

3.2.1 User controls

Controls are divided into the following categories: topology, signals, bus operations and car operations. Some of these features are available directly from the user interface, and some from the code.

Topological operations parameters include the number of segments, the number of lanes, the mean segment length and the coefficient of variation of segment lengths. Two corridor types can be selected: ring-corridors or regular corridors. For ring-corridors, an initial density is defined and vehicles do not appear or disappear, unless they can turn on network systems. Regular corridors have an entrance at the beginning of the corridor and an exit at the end of the corridor. Therefore, an inflow at the entrance is defined. Notice that density cannot be defined explicitly for these type of corridors. Finally, an option is available to choose between corridors or networks.

Signal parameters include mean green times, mean red times and a coefficient of variation parameter. All green and red times are realizations of a normal distribution with these parameters. For homogeneous corridors, an additional offset parameter needs to be defined.

Bus operational inputs are defined as the free-flow speed, the probability of stopping at each mid-block, and dwell times obtained from a normal distribution with a defined mean and coefficient of variation. Car operational parameters include the free-flow speed and lane-changing parameters such as the "look-ahead" value and the lane changing safety gap.

An additional essential parameter is the time aggregation period, which can be set directly by the user.

CHAPTER IV

BUS EFFECTS ON HOMOGENEOUS CORRIDORS

Homogeneous corridors have deterministic block lengths and signalization parameters and a homogeneous car vehicle class. Therefore, signalization patterns arise in time and space which makes it easy to determine MFD cuts. In this research, an additional bus vehicles class is introduced which introduced heterogeneity into the corridor. This creates complexities between the signalized intersections and the bottleneck effects created by buses. Homogeneous corridors are too simplistic compared to real-life corridors but can provide a basic framework to gain initial understanding on bus effects.

In the first section, homogeneous corridors are defined in more detail as well as their parameters. Then, a sensitivity analysis is performed using simulation to give an initial understanding of the problem. In the following section, a variational theory algorithm is presented which then helps to develop the analytical model.

4.1 Problem definition

Consider an urban ring-corridor with no turns having constant block lengths l, green phase duration g, cycle duration c, and signal offset o. Buses are introduced at the beginning of the corridor with inter-arrival times given by a Poisson process with mean μ_h. Buses travel on straight paths along the ring-corridors and do not make turns. They operate at free-flow speed, v, with a probability of stopping at each block p_s for a dwell time d. For each corridor realization at $t = 0$, a density k and a bus density proportion k_b/k is defined. Each vehicle on the network will then have a given probability of being a bus or a car based on this proportion. Vehicles on the corridor follow a triangular fundamental diagram, as defined by the kinematic wave

(KW) theory of traffic (35; 44), with free-flow speed $w^\sharp$, congestion wave speed $-w^\flat$, jam density κ, and saturation flow $Q = \kappa w^\sharp w^\flat/(w^\sharp + w^\flat)$.

Traffic conditions are measured by the MFD which is normalized by the capacity flow and jam density, giving quantity ranges between 0 and 1. The normalized values allow us to compare results with different number of blocks, block lengths, number of lanes, and time aggregations.

Following Laval & Castrillon (33), parameters are reformulated as dimensionless parameters. This reduces the number of inputs and helps to generalize findings. Topological parameters are defined:

$$\lambda = l/l_c, \;\; l_c = \frac{g}{1/\omega^\sharp + 1/\omega^\beta} \tag{18a}$$

$$\rho = r/g \tag{18b}$$

Here, λ is the block length, ρ is the red to green ratio, $\omega^\sharp$ is the free-flow car speed and ω^β is the congestion wave speed. An additional parameter is used to describe the signal offset:

$$\tau = o/c. \tag{19}$$

Notice that τ's will vary between 0 and 1. Finally, two parameters are used to describe bus parameters:

$$\gamma = h/g, \tag{20a}$$

$$\alpha = \tilde{v}/\omega^\sharp, \tag{20b}$$

where γ is the dimensionless headway and α is the dimensionless average free-flow speed normalized by the car free-flow speed.

4.2 Simulation sensitivity analysis

An initial simulation experiment is performed to examine the sensitivity of the MFD to input parameters. Twenty-seven roadway cases with one lane are considered, which

are obtained by combining three different λ values (0.5, 1, 1.5), ρ values (0.5,1.0,1.5), and τ values (0,0.3$\overline{3}$,0.6$\overline{6}$). Nine cases are shown on Figure 10 for clarity, but the following findings are general:

a) The "NO BUS" case provides an MFD upper bound to cases with buses. This upper bound is tight during congested regions, but usually not tight during free-flow or capacity regions. This suggests that existing analytical methods, which do not consider buses, overestimate flow.

b) Bus operations shift the MFD to the right during free-flow and near-capacity regions. This effect is similar to the moving bottleneck effect that has been observed on freeways.

c) As bus headway increases the capacity is reduced. This effect cannot be explained by the moving bottleneck effect and is likely coming from the short-block effect.

d) The effect of bus headway on the MFD varies greatly depending on corridor configuration. As ρ increases, the flow decreases for all bus headways, as expected. As λ and τ changes, the MFD shape changes drastically. This phenomena can be explained as offsets create red phase bands, or "red waves", that propagate through the system and resemble a moving bottleneck. Therefore, if bus trajectories are having to stop at every red signal on a red wave, then the effect of buses will be negligible; e.g.; see case $\lambda == 0.5$, $\rho = 1.5$ and $\tau = 0.33$. The interaction of the red wave and the buses will create very different MFD shapes.

4.3 Theoretical Methods

Two models are presented in this section. The first is a variational theory algorithm which is modified from existing methods. The second is analytical and is developed

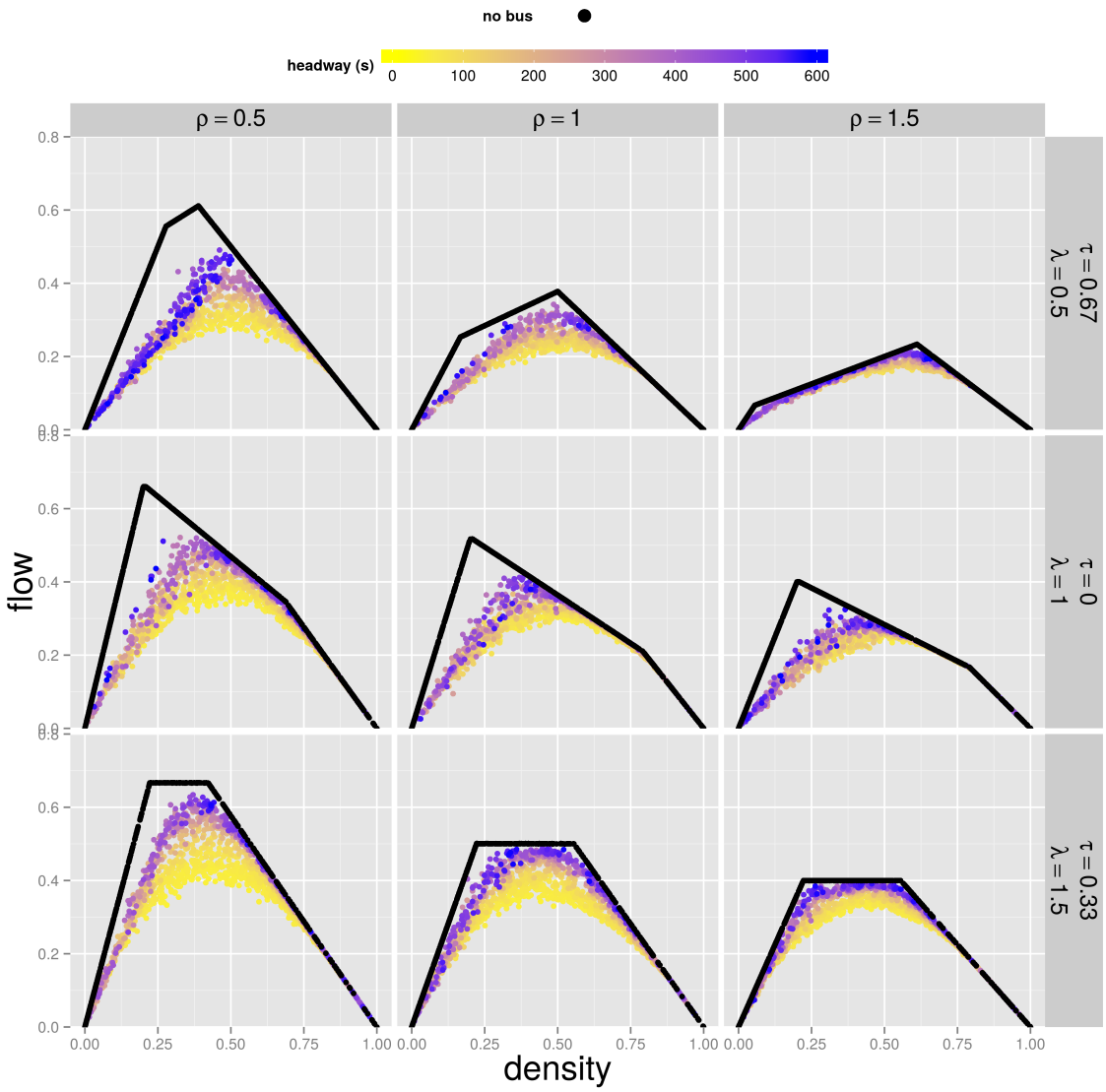

Figure 10: Sensitivity analysis of input parameters using simulation. Each diagram represents a different corridor configuration by varying topological network parameters λ, ρ, and τ. Every point on the diagram represents a corridor with varying vehicle density and bus headway. Additional parameters include: $g = 36$ s, $v = 60$ km/h, $p_s = 1/3$, $d = 30$ s, $b = 30$ blocks, $n = 1$ lanes.

using insight from the first model and from the simulation results on the last section. The following subsections describe the models and compare their predictions to simulation results.

4.3.1 Modified variational theory algorithm

Recall that variational theory problems can be formulated as shortest path problems on a graph network (10; 16). Xie et al.(49) extend this method by introducing buses with a linear trajectory traveling with an average speed throughout the corridor. The local capacity is reduced by one lane for any time period that the bus is active on a street segment. Building upon this model, a few modifications are made on this research by introducing bus trajectories endogenously as in Boyaci et al. (5). Bus trajectories are simulated throughout the network by operating at the running speeds and making stops when encountering a red phase or a bus stop; see Figure 11(a). Notice that obtaining running speeds is difficult because they are dependent on the level of traffic congestion. Therefore, buses are modeled using free-flow speeds as an approximation method.

The variational theory time-space graph network is built by defining an initial boundary and a generic point P in space, see fig. 11. The four types of links on the graph are described below:

- Red phase links with zero speed and zero maximum passing rate.
- Connecting links that start at the beginning and end of a red phase, travel with free-flow speed u or congested wave speed $-w$, and stop when another red phase is encountered. Maximum passing rates are given by $Q - k_C s$ for a wave speed s, where C is the capacity state of the triangular fundamental diagram.
- Bus stops with zero speed and maximum passing rate defined by the number of lanes that the bus is not blocking: $Q\frac{n-1}{n}$.

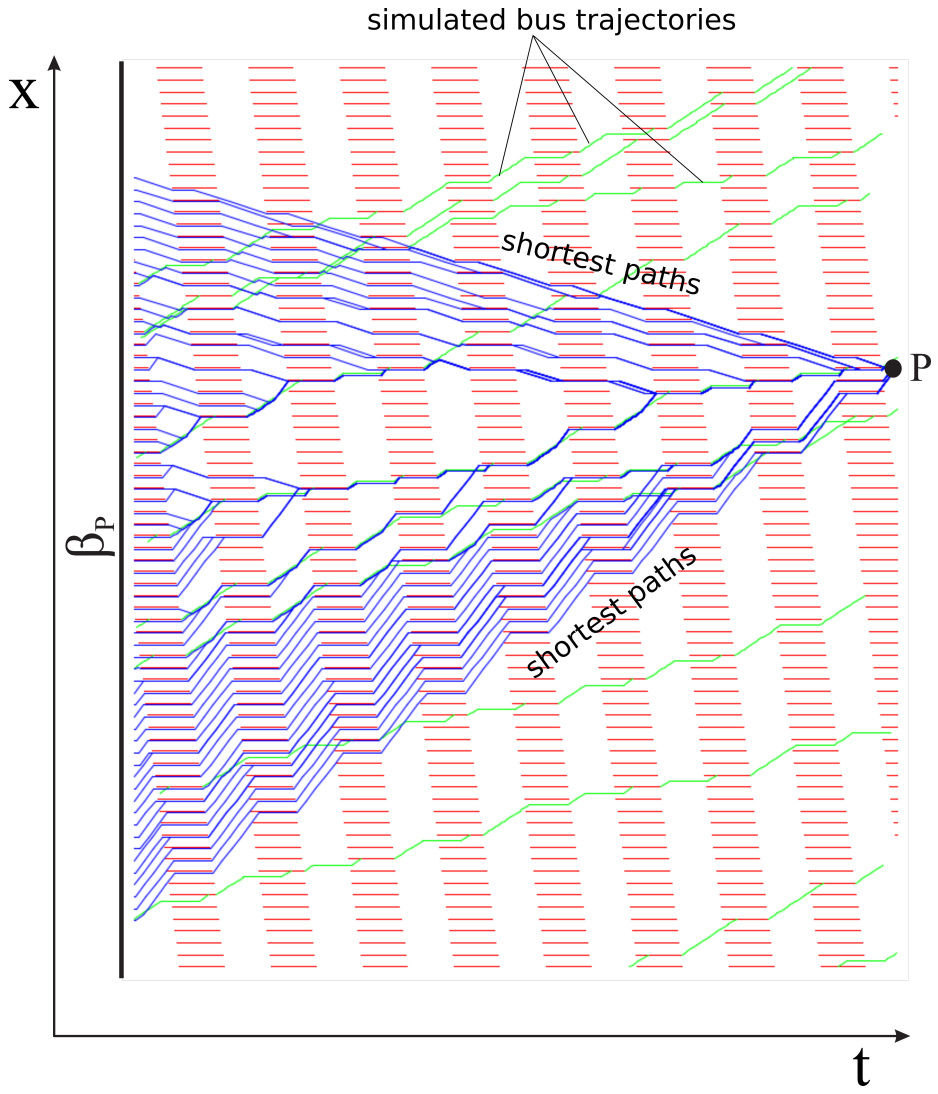

Figure 11: (a) Traffic states generated by a moving bottleneck; (b) visual representation of the VT method, simulated bus trajectories are represented by green lines

- Running bus links with free-flow speed v and maximum passing rate equal to $Q_D - k_D v$ where $k_D = Q_D/u$ represents the downstream density

Each shortest path from the boundary to P will have an average passing rate and an average speed which is used to construct an MFD upper boundary cut. an experiment is performed to test the accuracy of the modified VT algorithm relative to the simulation. The results on Figure 12 suggest the following:

a) The method provides an accurate upper bound approximation to the MFD.

b) The corridor can be modeled using endogenous bus trajectories operating at free-flow speeds even as these speeds are not maintained when queues begin forming during congestion.

4.3.2 Analytical method

An analytical method is developed using insight from simulation and variational theory experiments. From simulation results, it is found that the "no bus" MFD is an upper bound to the MFD when buses are introduced. However, this upper bound is not tight for regions of free-flow and near-capacity. Therefore, the approach is to consider the "method of cuts" for the "no bus" case and add two more cuts to account for the flow reduction from bus operations. Variational theory helps us to evaluate two major effects, the moving bottleneck effect and the short-block capacity effect, which correspond to the added "bus cuts".

4.3.2.1 Moving bottleneck cut

Simulation results suggest that moving bottlenecks effect is present on signalized corridors. In order to test this hypothesis, the moving bottleneck "cut" is evaluated using a variational theory framework. A bus trajectory traveling at free-flow conditions is assumed similar to the method from last section. In order to estimate the MFD cut, an average speed and a maximum passing rate of this trajectory is evaluated.

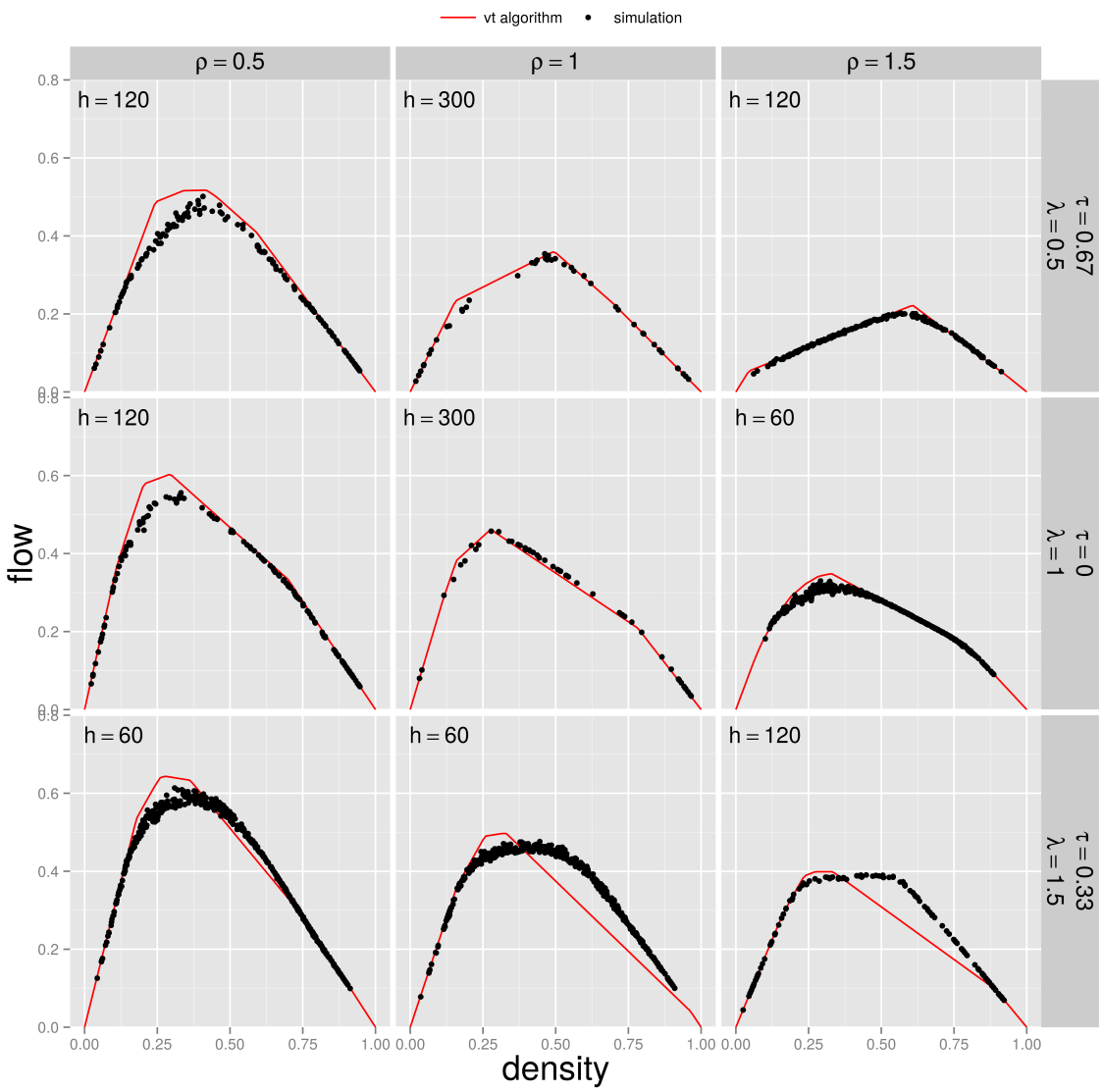

Figure 12: Comparions of modified VT method and simulation. The same ρ, λ values are used from the simulation experiement, but only one γ and τ value is shown for each case. The remaining parameters are: $b = 30$ blocks, $g = 36$ s, $v = 60$ km/h, $p_s = 1/3$, $d = 30$ s, $n = 2$ lanes.

Obtaining average free-flow speeds is a tedious task since one must consider travel delays from bus stops and traffic signals. These vary widely depending on the configuration of the network and a simple formula is not easily attainable. In order to overcome this, two bus trajectories are considered. One trajectory travels on an unsignalized corridor with bus stops being the only delays. The second trajectory considers a signalized corridor but does not make any bus stops. The speed estimate is calculated using a harmonic average of the two speeds.

A renewal reward process is applied to estimate average speeds. First, consider a renewal "cycle" i where a bus travels with free-flow speed v for distance L_i across N_i blocks, then stops at a traffic signal or a bus stop for time S_i, waits for the duration of the stop and ends the cycle. Then, another cycle begins with the free-flow speed. Notice that the sequence of elapsed times T_i, $i \geq 1$ for each cycle i are independent and identically distributed and are equal to $N_i l/v + S_i$. The "reward" for each cycle is defined as the distance traveled L_i, $igeq1$ which is also i.i.d. The distance traveled on each cycle depends on the number of street segments N_i traveled before making a stop. Since segment lengths are deterministic at, then the length is obtained by $L_i = N_i l$. The main result of renewal reward theory is that the average speed $\tilde{v}$ can be calculated by the expected reward divided by the expected duration of each cycle:

$$\tilde{v} = \mu L/\mu T = \frac{\mu_N l}{\mu_N l/v + \mu_S}. \tag{21}$$

For the first case, where delays are given by bus stops, all variables are denoted with an "A" subscript. The number of street segments traveled before making a stop is modeled as a geometric a process with mean $1/p_s$, which gives:

$$\mu_{N_A} = 1/p_s, \tag{22a}$$

$$\mu_{S_A} = d. \tag{22b}$$

For the second case, where buses do not make stops, variables are deterministic due to repetitive nature of homogeneous corridors. These are defined with a "B" subscript

and have been formulated by the the fastest cut of the "method of cuts" (15):

$$\mu_N^B = 1 + max\{N : [N(l/v - o + c)] \mod c \leq g/c\}, \tag{23a}$$

$$\mu_S^B = c - [N_{max}(l/v - o + c)] \mod c, \tag{23b}$$

where o is the offset time and c is the cycle time.

Average free-flow speeds for both cases, w_A and w_B, can now be readily obtained from 4.3.2.1. Now, the average bus speed $\tilde{v}$ is estimated from a harmonic average of the two cases:

$$\tilde{v} = 2/\left(1/w_A + 1/w_B\right) \tag{24}$$

Finally, results are generalized by estimating a dimensionless average bus speed α normalized by the free-flow car speed:

$$\alpha = \tilde{v}/w^\sharp \tag{25}$$

In order to test this approximation method an experiment with 1000 points is run. True speed values are generated from simulated bus trajectories throughout a corridor with 200 blocks and estimated values are obtained from eq. 4.3.2.1. For each run, random input variables are generated for each of the parameters. Four of the parameters are uniformly distributed: $\lambda \epsilon \{0.25, 2.25\}$, $\rho \epsilon \{0.2, 2\}$, $\tau \epsilon \{0, 1\}$, and $\gamma \epsilon \{0, 24\}$. Also, average bus speeds cannot be implicitly defined so bus input parameters are drawn. These are also uniformly distributed with ranges $p_s \epsilon \{0, 1\}$ and $d \epsilon \{0, 60\}$ sec, while v can only take four discrete values $\{20, 40, 60, 80\}$ km/h. The results on Figure (13) suggest that the method to estimate average speeds provides a reasonable approximation.

The next step is to calculate maximum passing rates from shortest paths. This is not a straightforward task since paths are unpredictable due to the interaction between traffic signals and bus trajectories as has been observed on fig. 12. In order

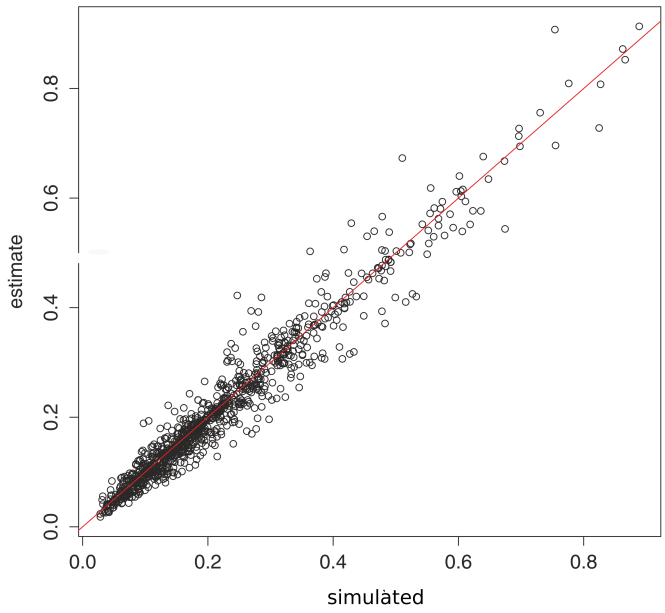

Figure 13: y-y plot of "simulated" vs. "estimated" α speeds

to overcome this, the corridor is separated into two lane types: a mixed car-bus lane and $n-1$ car-only lanes. The assumption is that at any given location there is no more than one bus on all lanes, which is reasonable since buses usually operate and make stops on the outside lane. The advantage of separating the corridor is that for the mixed lane, the maximum passing rate for the moving bottleneck is zero, since no cars can overtake buses on that lane. Therefore, shortest paths will always follow bus trajectories since they provide the minimum cost available. Also, the maximum passing rate on a car-only lane can be readily obtained by estimating the "method of cuts" and placing a line with slope $\tilde{v}$ tangent to the MFD curve. Then the y-intercept of the curve provides the passing rate; see fig. 4.3.2.1. Notice on the figure, that if a discontinuity is present the line will intersect the discontinuous point; see, e.g. point "1" on Figure 4.3.2.1. The final maximum passing rate for all lanes is the weighted average of the two lane types:

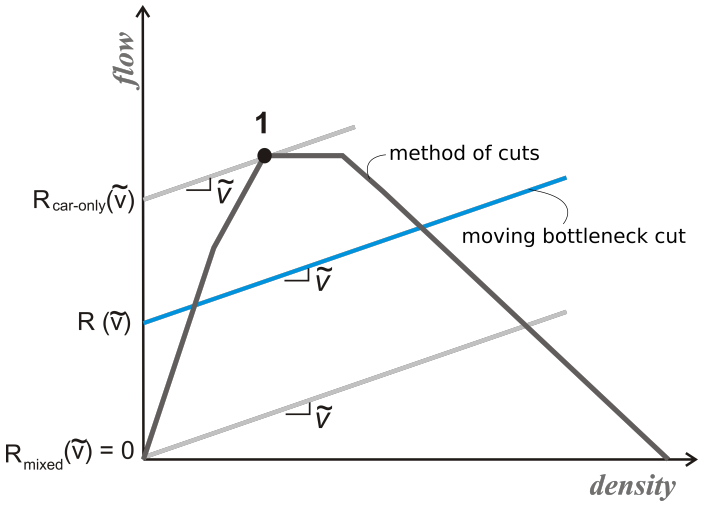

Figure 14: The moving bottleneck cut can be constructed using a lane weighted average of the maximum passing rate (R) from mixed lanes and car-only lanes.

$$R(\tilde{v}) = \frac{1}{n} R_{mixed}(\tilde{v}) + \frac{n-1}{n} R_{car-only}(\tilde{v}) \tag{26}$$

Where $R_{mixed}(\tilde{v})$ is the maximum passing rate of the mixed car-bus lane with average speed $\tilde{v}$, $R_{car-only}(\tilde{v})$ is the maximum passing rate of the car-only lane, and n is the number of lanes.

4.3.2.2 Capacity reduction from the "short block" effect

Estimating the capacity cut of a corridor with buses is challenging because of the unpredictable interactions created by the short-block effect. A regression model is employed to estimate this particular cut. The regression is based on variational theory experiments for the single mixed car-bus lane. The inputs of the model include topological parameters λ, ρ and τ and bus parameters γ, α. In order to develop the model, 1000 different training runs and 500 testing runs are created with the equal input variable distributions defined on the previous subsection. additionally, the dimensionless average bus speed α is estimated from eq. 4.3.2.1.

Each run consists of a variational theory graph with the defined inputs. For each, a shortest path is obtained which begins and ends at the same location. The

maximum passing rate of the shortest path provides the short-blcok capacity Q_{mixed} of the mixed lane. The final regression equation is obtained by adding all relevant variables and keeping the significant ones at the 0.001 level:

$$Q_{mixed} = a_1\alpha - a_2\alpha^2 + a_3\alpha^3 + a_4\lambda - a_5\rho\alpha + \log(\gamma^{a_6}) \tag{27a}$$

where $a_1 = 2.781282$, $a_2 = 4.328240$, $a_3 = 2.589717$, $a_4 = 0.032333$, $a_5 = 0.544471$, and $a_6 = 0.034573$.

For the test data, the mean absolute error is 0.039 and the root mean square error is 0.0464 (Recall that capacity ranges from 0 to 1). Notice that the dimensionless offset τ is not a significant variable, and the model only requires the remaining four parameters.

The model suggests that α has a cubic polynomial effect on capacity as well as an interactive effect with ρ. Also, λ has a positive linear effect and γ has a positive logarithmic effect on capacity. The marginal effect of the input parameters is given on the first row of Table 1. The variable ρ has a negative marginal effect, which is expected since the red phase increases compared to the green phase. Also, λ has a positive marginal effect which is expected since the queues from bus stops have a larger block length before they spill back to upstream intersections. Furthermore, γ has a positive marginal effect on capacity which is also expected since an increase in headway translates to a decrease in the number of buses on the corridor.

The last row of the table gives the elasticity of input parameters evaluated at their mean values. The results suggest that ρ and α are the most important parameters when determining capacity at the mean input values.

Finally, to estimate the capacity of all lanes, we obtain the capacity of the mixed lane from eq. 27 and the capacity of the car-only lanes from the "method of cuts"; see Figure 4.3.2.1. The final equation is:

$$Q = \frac{1}{n}Q_{mixed} + \frac{n-1}{n}Q_{car-only} \tag{28}$$

	$x = \rho$	$x = \lambda$	$x = \gamma$	$x = \alpha$
$\frac{dQ_{mixed}}{dx}$	$-a_5\alpha$	a_4	a_6/γ	$a_1 - 2a_2\alpha + 3a_3\alpha^2 - a_5\rho$
mean of x	1.053	1.229	11.924	0.224
x-elasticity of Q_{mixed}	-0.298	0.092	0.080	0.341

Table 1: Marginal effect and elasticity of inputs

4.3.2.3 Results

In this experiment we investigate the accuracy of the analytical method relative to the traffic simulation. The results on Figure 15 suggest the following:

a) The two added "bus cuts" are sufficient to create a tight approximation to the MFD.

b) The moving bottleneck effect is verified for urban corridors as the cut provides a tight upper bound to the MFD. Notice that the cut is evaluated at free-flow speeds even as these speeds are not maintained when congestions is present.

c) The short-block effect is essential when considering multimodal corridors and can be captured by the corresponding cut. To the author's knowledge, no one has analyzed this effect in the context of urban operations.

d) The MFD can be modeled by using the dimensionless average speed α while ignoring inputs such as the bus free-flow speed v, the stop probability p_s and the dwell time d. This helps to reduce the number of parameters.

4.3.3 Discussion

The main result of this chapter is that buses create two major effects on corridors: the moving bottleneck effect and the short-block effect. The modified VT method and the developed analytical method are able capture these effects accurately. However,

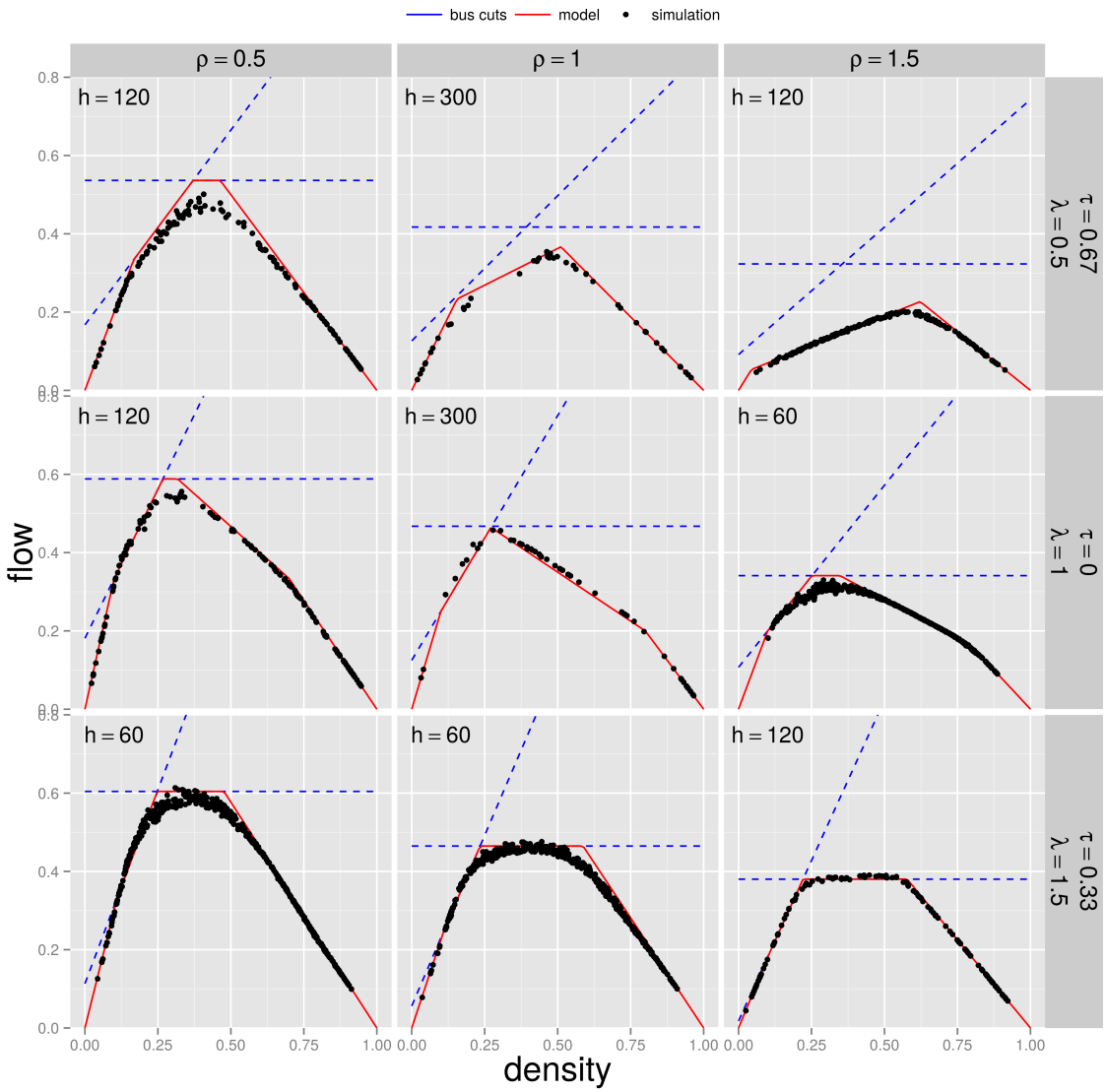

Figure 15: Comparions of the analytical method to simulation results. The same ρ, λ are used from Experiment 1, but only one γ and τ value are used for each roadway case. The remaining parameters are: $b = 75$ blocks, $g = 36$ s, $v = 40$ km/h, $p_s = 1/3$, $d = 20$ s, $n = 2$ lanes.

the analytical method is much simpler to apply as it requires only four parameters and provides valuable insight. The model finds that the red to green ratio ρ and the dimensionless average bus speed α have the largest effect on corridor capacity when evaluated at mean values. Finally, this model is dimensionless and does not have to be re-calibrated for each roadway configuration.

This study considers ring corridors, but often boundaries are present that can affect the MFD. For instance, consider a corridor that has entrances and exits on fig. 16(b). Bus trajectories will create boundary effects on buses that are significant. The simulation results on 16(a) shows that the MFD changes depending on the number of blocks on the corridor. For a short corridor, boundary effects correspond to a higher flow during free-flow and near-capacity regions. For long corridors, results converge as boundary effects are diminished and results become similar to ring-corridors. These boundary effects must be evaluated in future research.

This research constitutes an initial step in understanding multimodal corridors performance. The research assumes simplistic operations and stochastic behavior is the next logical step.

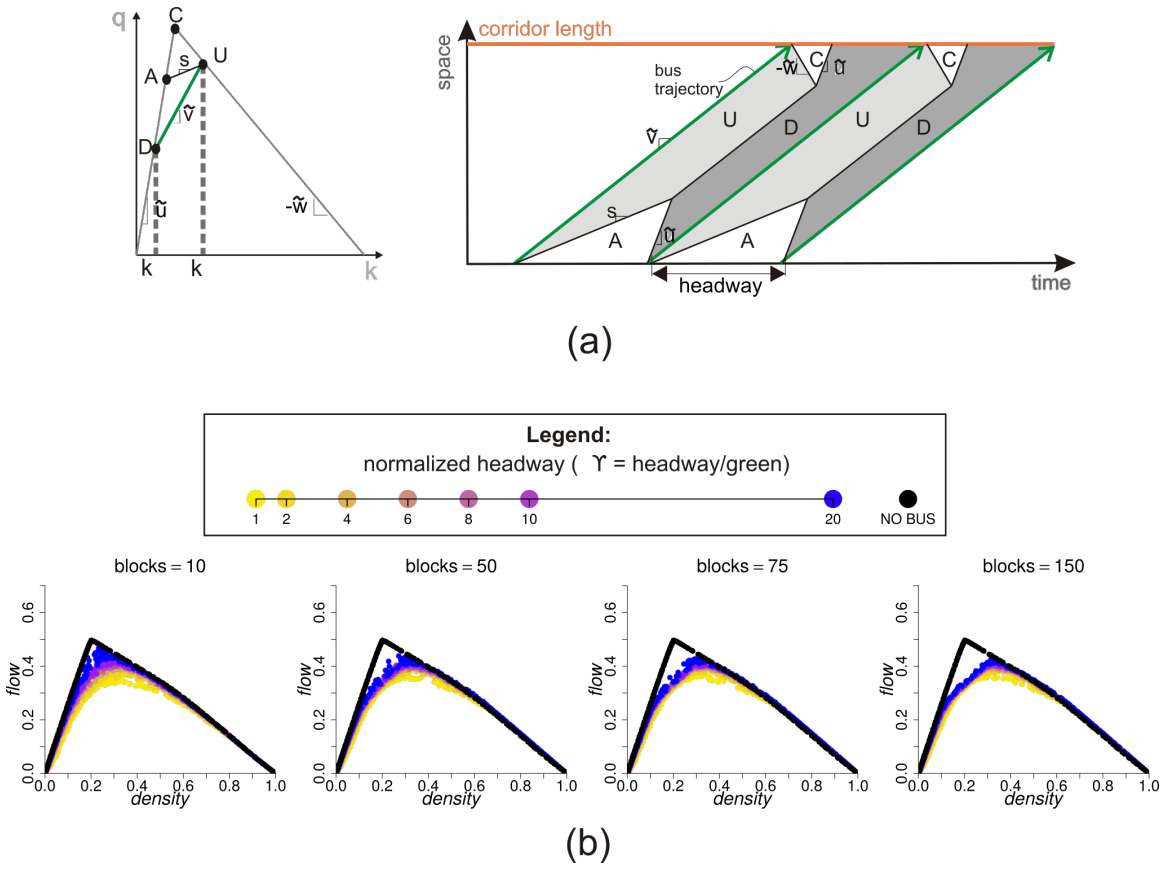

Figure 16: (a) Simulation runs with varying number of blocks. The input parameters are: $\lambda = 1.0$, $\rho = 0.5$, $\tau = 0$, $g = 30$ s, $v = 30$ km/h, $p_s = 1/3$, $d = 20$ s, $n = 2$ lanes. (b) Kinematic wave time-space diagram example showing the boundary effects of buses. Notice that for an input flow "a", there are boundary effects "a" at the beginning of the corridor and "C" at the end of the corridor. Speeds with a "tilde" denote average macroscopic quantities.

CHAPTER V

BUS EFFECTS ON STOCHASTIC CORRIDORS

Stochastic corridors are more complex than homogeneous corridors as street segment lengths and signalization parameters vary over time. This makes the MFD of stochastic corridors more difficult to evaluate. As buses are introduced, the interactions between buses and signalized intersections create very complex behavior in traffic dynamics. In this chapter, the MFD of stochastic corridors with buses is evaluated.

The first section describes the problem in more detail. Then the analytical model is developed in two parts: the bus short block effect and the moving bottleneck effect. Finally, model outputs are compared to simulation results and a brief discussion is presented.

5.1 Problem definition

Consider a ring-corridor with B street segments of varying lengths delimited by traffic signals whose red and green times vary by time and distance. This corridor is a realization of a "stochastic corridor" random variable, where each segment length, green time, and red time are obtained from random variables l, g, r respectively. The variables are i.i.d. with mean $\mu_{\_}$, standard deviation $\sigma_{\_}$, and coefficient of variation (cov) $\delta = \mu_{\_}/\sigma_{\_}$ where "$\_$" is a placeholder for any of the random variables. It is assumed that the cov for all random variables are equal, $\delta = \delta_l = \delta_g = \delta_r$. Vehicles on the corridor follow a triangular fundamental diagram, as defined by the kinematic wave (KW) theory of traffic (35; 44), with free-flow speed $w^\sharp$, congestion wave speed $-w^\flat$, jam density κ, and saturation flow $Q = \kappa w^\sharp w^\flat/(w^\sharp + w^\flat)$.

Buses travel on straight paths along ring-corridors and do not make turns. Buses

have a free-flow speed, v, probability of stopping at each block p_s, and a dwell time random variable d obtained from a normal distribution with mean μ_d and cov δ. A bus that is not making a stop can pass another bus that is making a stop on the inside lane. For each corridor realization, initial boundary conditions are defined by specifying a vehicle density k and a proportion of buses k_b/k where k_b is the bus density. Each vehicle on the network will then have a given probability of being a bus or a car based on this proportion.

5.2 Multimodal corridor MFD model

Bus operations reduce corridor flow and thus existing models overestimate the MFD flow. Using the VT framework, shortest paths are altered by the presence of bus trajectories, as shown in fig. 17. Notice that this creates very complex behavior where paths take unpredictable paths which are difficult to model. A few extensions are added to the corridor MFD model to account for these effects. Please refer to the background section for the theory behind the model. Similar to the homogeneous corridor on the last chapter, moving bottleneck and short-block effects are considered.

5.2.1 Sensitivity Analysis

In this section a sensitivity analysis is performed on nine different stochastic corridors each with varying input parameters. The goal is to analyze how the λ, ρ, and headway inputs influence the MFD when other parameters are held constant. The results on fig. 18 provide the following findings:

1 As the dimensionless segment length λ increases, the MFD flow increases. This is expected since longer segments provide more vehicle storage which helps to limit queue propagations to upstream intersections.

2 As the red/green ratio ρ increases, the MFD flow decreases. This is expected since more red time compared to green time reduces intersection capacity.

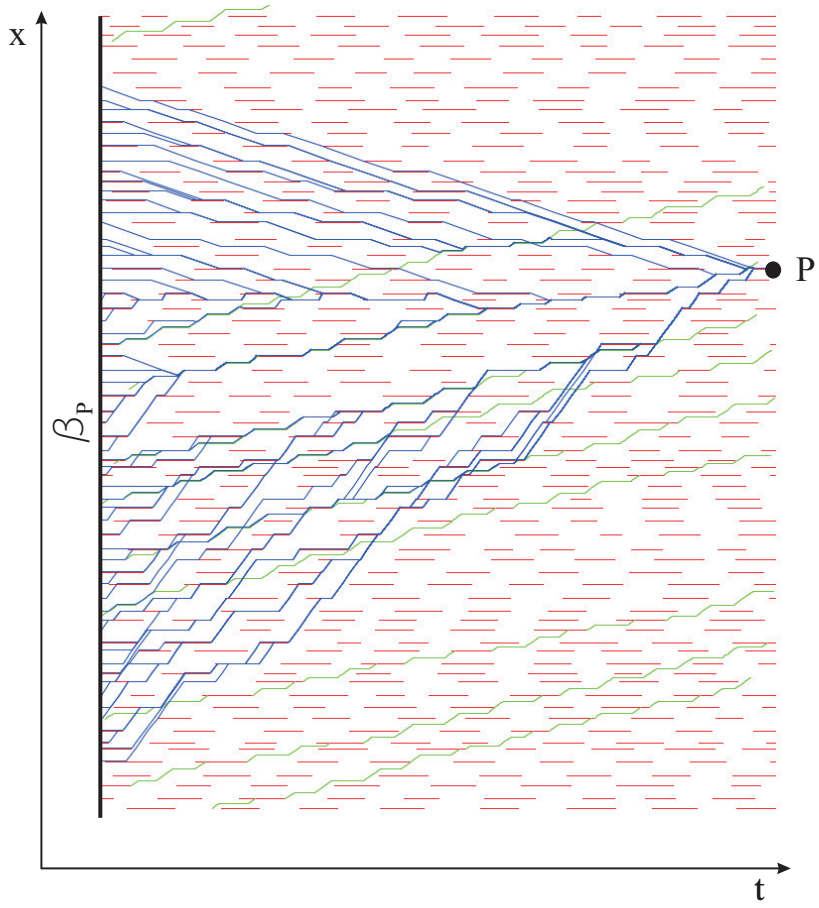

Figure 17: VT graph shows minimum paths (in blue) starting at the boundary β_P and ending at P being altered by bus trajectories (in green) or red singnals (in red)

3 As headways increase, the MFD flow also increases as expected. More interestingly, the effect of buses is greater when the red/green ratio is smaller. A possible explanation for this is that the effect of buses is reduced by the effect of red signals. Therefore, the larger red times become, the more that the bus effect is mitigated.

4 The transformed MFD loses its symmetric property when buses are introduced. This is likely due to the moving bottleneck effect which skews the diagram to the right. This effect is investigated further in this chapter.

5.2.2 Modeling buses as stationary bottlenecks

Bus operations create a short-block effect as they interact with traffic signals and reduce the MFD as previously seen on fig. 7(d). Instead of trying to model these unpredictable interactions, the effects are estimated with stationary bottlenecks which temporarily reduce the capacity of nearby intersections. This has proven to be a good approximation (16; 49), but has not been formulated analytically with respect to MFD theory.

Consider a bus trajectory with average speed ω^{avg} traveling through an unsignalized corridor from point A to point B as shown on fig. 19(a). Notice the three alternative paths from A to B, consisting of piece-wise linear links taking either speed $w^{\#}$ or 0, where horizontal links are stationary bottlenecks blocking one lane. Previous research has shown that the three alternative paths have an equal passing rate to the bus trajectory path. This result is used to replace bus moving bottlenecks with a method similar to "alternative path 1", where a stationary bottleneck is placed at the downstream intersection of each street segment. Notice that the stationary bottleneck could realistically be located anywhere along each segment, but placing it at the intersection eliminates short-block effects which are complex to model.

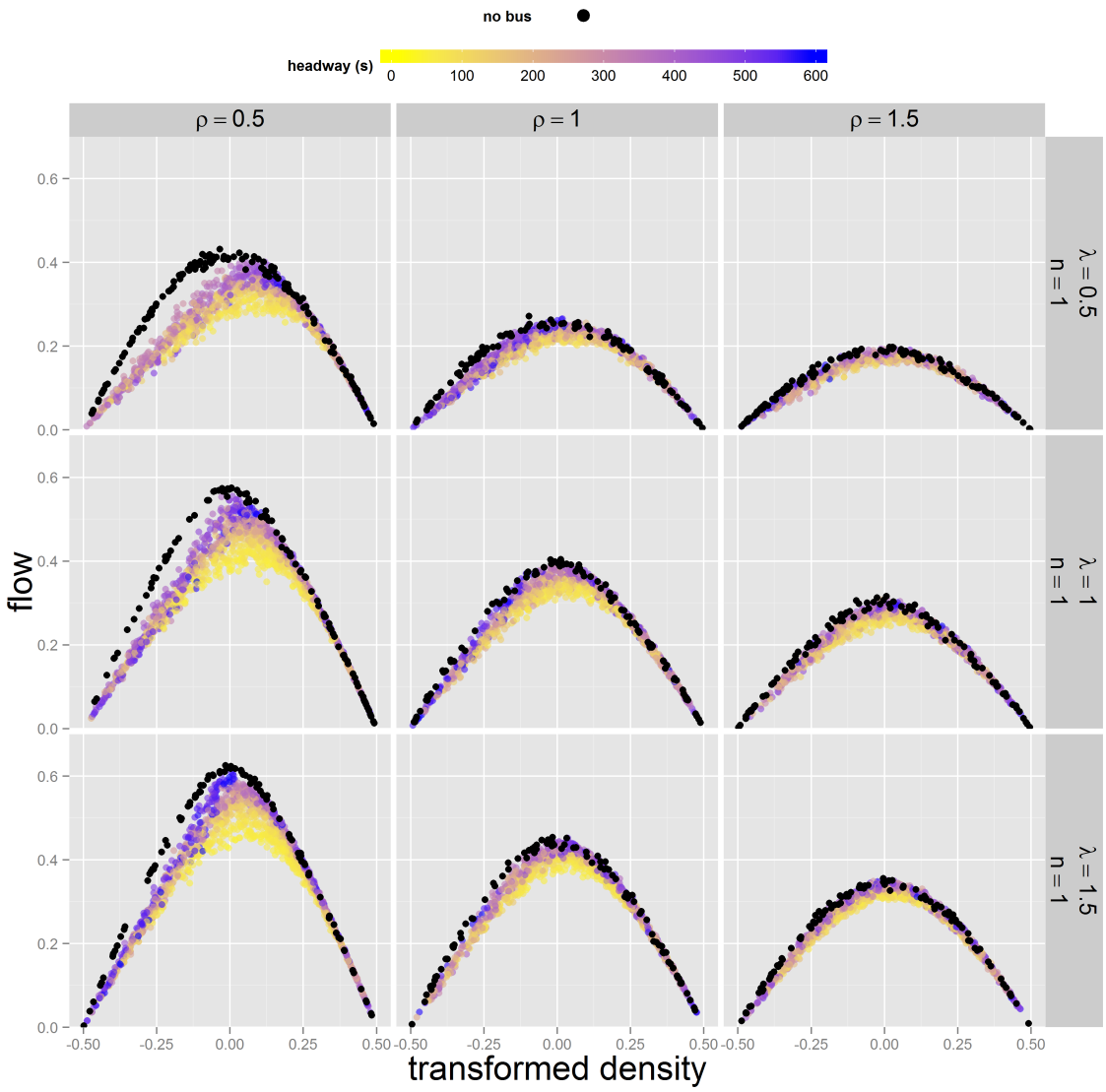

Figure 18: Sensitivity analysis of stochastic corridors using simulation. Each diagram represents a different corridor configuration by varying topological network parameters λ and ρ. Every point on the diagram represents a corridor realization with varying vehicle density and bus headway. Additional parameters include: $g = 36$ s, $v = 60$ km/h, $p_s = 1/3$, $d = 30$ s, $b = 30$ blocks, $n = 1$ lanes.

If more than one bus is considered along a street segment, stationary bottlenecks have a similar behavior compared to traffic signals as shown in fig. 19(b). The red signal times $\bar{r}$ consist of the bottleneck durations, the cycle time is the inter-arrival time between two buses, and the green time $\bar{g}$ is the leftover cycle time minus the red time duration. This signal-like effect created by the stationary bottlenecks is called the "bus signal" for the remainder of the chapter. Red phase durations are obtained by the time it takes a bus to travel through a segment plus the dwell time minus the time traveled by the upstream free-flow wave:

$$\bar{r} = l_i(1/v - 1/w^\sharp) + D_{i,j}. \tag{29}$$

In the above equation, $\bar{r}$ is the bottleneck duration, l_i is the length of street segment i and $D_{i,j}$ is the dwell time duration of bus j in segment i. The dwell time can be formulated as:

$$D_{i,j} = dy, \quad \text{where} \qquad y = \begin{cases} 0 & \text{w. prob. } 1 - p_s \\ 1 & \text{w. prob. } p_s \end{cases} \tag{30}$$

where d is the distribution of the dwell time. By conditioning on y, the mean and variance of D can be obtained:

$$\mu_D = \mu_d p_s, \tag{31a}$$

$$\sigma_D^2 = p_s\left(\mu_d^2(1 - p_s) + \sigma_d^2\right) \tag{31b}$$

One assumptions that is made is that buses operate on only one of the lanes, called the "mixed lane" which has proven to be a good approximation for homogeneous corridors. Therefore, an intersection has two types of stationary bottlenecks coming from the "traffic signal" blocking all lanes, and the "bus signal" blocking the mixed lane. In order to differentiate between the two signal types, the parameters from the bus signal are denoted with an overbar, i.e. $\bar{g}$, $\bar{r}$, $\bar{\rho}$, the parameters for the traffic signal are left unchanged; i.e. g, r, ρ; and effective parameters for all lanes are given

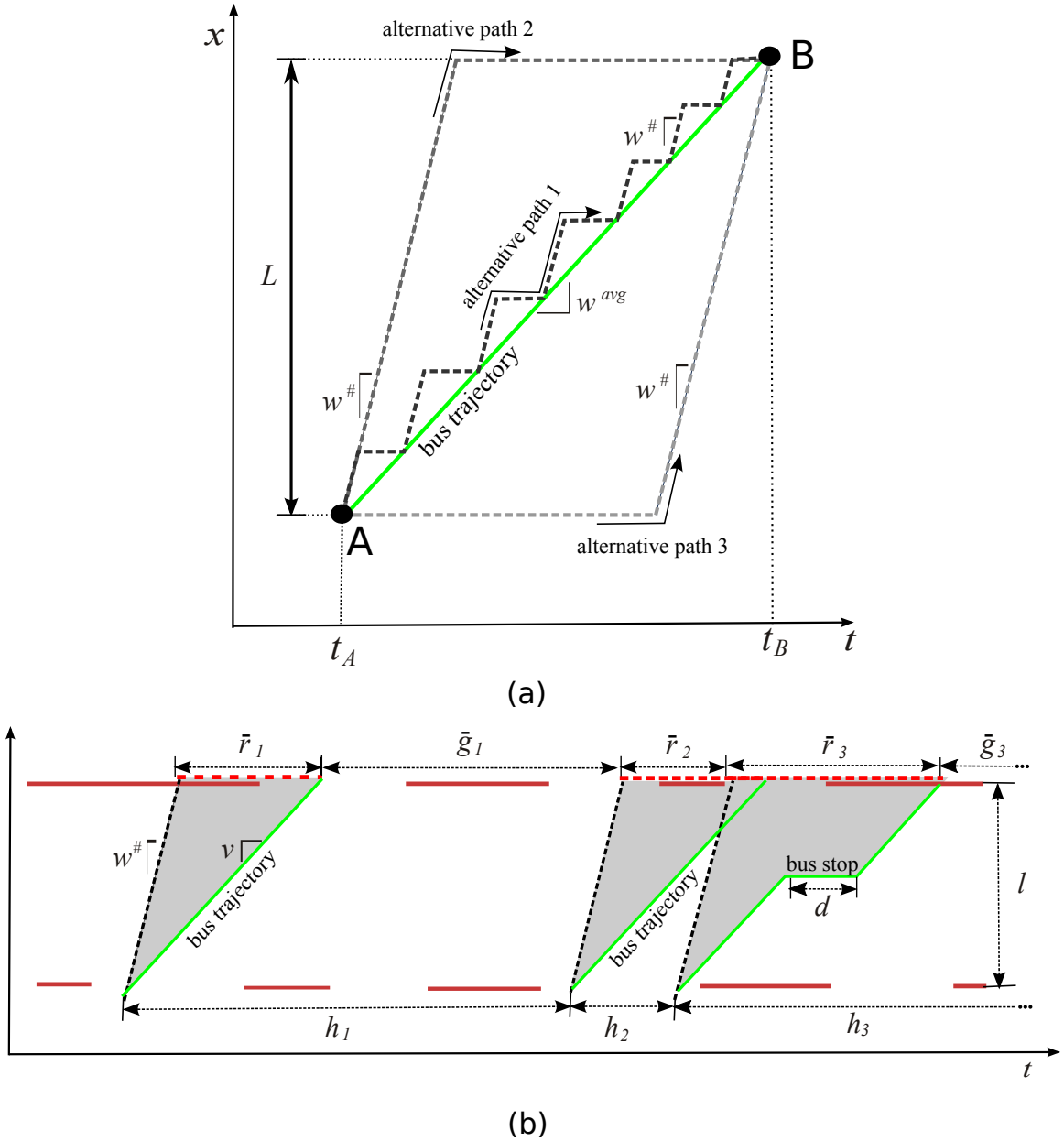

Figure 19: (a) alternative paths have equal average speed and passing rate than the bus trajectory. (b) Buses traveling through a street segment create a signal-like effect at the downstream intersection

with an "e" subscript; i.e. g_e, r_e, ρ_e. Effective values help to combine the effects of both signal types into one set of parameters. These are estimated by taking into account the events where the intersection is constrained or unconstrained by bus or signal bottlenecks. Therefore, effective red times are defined as the events where either the traffic signal or the bus signal are red, and effective green times as the events where both signals are green. The green and red proportions are first derived for the two signal types before analyzing effective values.

The long-run red proportion for traffic signals and bus signals are denoted by P_r and $P_{\bar{r}}$ respectively. Evaluating these proportions is done with an alternating renewal process (45) which considers two alternating states, "green" and "red". The process begins at state "green" for duration g_1, then changes to "red" for time r_1, then goes back to "green" for g_2, then "red" for r_2, and so on. The distributions of the duration of the "green" and "red" times g_i and r_i can differ but the sequence of random variables g_i and r_i, for $i \geq 1$ must be independent and identically distributed. Conditions are satisfied since for every signal cycle i, the distributions for red and green times are identical. The alternating renewal reward process gives the following long-run proportions of red time to total time:

$$P_{\bar{r}} = \frac{\mu_{\bar{r}}}{\mu_{\bar{r}} + \mu_{\bar{g}}}, \tag{32a}$$

$$P_r = \frac{\mu_r}{\mu_r + \mu_g}, \tag{32b}$$

where $\mu_{\bar{r}} = \mu_l(1/v - 1/w^{\#}) + p_s d$ and $\mu_{\bar{r}} + \mu_{\bar{g}} = \mu_h$. Notice that green time proportions are easily obtained by $P_{\bar{g}} = 1 - P_{\bar{r}}$ and $P_g = 1 - P_r$. Now, since the traffic signal and the bus signal are independent of each other, the long-run proportion of effective green and red times is obtained by using proportions as probabilities in time. The effective long-run values are obtained from the addition rule of probability:

$$P_{r_e} = P_{\bar{r}} + P_r - P_{\bar{r}} P_r, \tag{33a}$$

$$P_{g_e} = 1 - P_{r_e}, \tag{33b}$$

where P_{r^e} and P_{g^e} are the effective red and green proportion for the mixed lane. The long run red/green ratio is altered by the change in red and green proportions, and is now denoted by subscript m representing the mixed lane:

$$\rho_m = P_{r_e}/P_{g_e} = \rho + \bar{\rho} + \rho\bar{\rho}. \tag{34}$$

In the above equation, ρ is already known, but for the bus signal the value is obtained by dividing the red and green proportions:

$$\bar{\rho} = P_{\bar{r}}/P_{\bar{g}} = \left[\frac{1}{\mu_l(1 - w^\sharp/v) + p_s d} - 1\right]^{-1} \tag{35}$$

The next step is to obtain the red/green ratio for the corridor with n lanes. Consider that $n-1$ lanes are unaffected by the buses and maintain their original red/green ratio. Taking a weighted average based on all lanes, the ratio becomes:

$$\rho_e = (\rho)(n-1) + (\rho + \bar{\rho} + \rho\bar{\rho})(1) = \rho + \bar{\rho}/n + \rho\bar{\rho}/n. \tag{36}$$

The effective value is now used as the new ρ value for the corridor MFD model. Notice that the new effective value will affect all MFD cuts and not only the short-block cut.

5.2.3 Moving bottleneck cut

Stationary bottlenecks are not sufficient to capture the cut that is generated by moving bottleneck trajectory. The reason being that the bottlenecks from the "bus signals" are assumed to be random and independent across time and distance, while buses follow specific trajectories throughout the network. Therefore, the aim of this cut is to capture the time-space correlation created by the bus trajectory across the time-space diagram. Toward this end, bus trajectories are modeled as a renewal rewards process similar to the strategies used for the corridor MFD model. It is assumed that buses travel at free-flow speeds which has proven to be a good approximation for homogeneous corridors.

Consider a bus that travels from boundary β to point P on a corridor with n lanes and only stops when encountering a red signal or a bus stop. Notice that if this path is traced backwards in time starting from point P and traveling to a point B in β, the path follows a similar renewal rewards process compared to routing strategy s_1^ω from the stochastic corridor MFD model except that the vehicle is traveling with bus free-flow speed v and making bus stops. Thus, each renewal cycle i begins at the start of a red signal, travels backwards in time with speed $-v$ for a time T_i a length L_i and a number of blocks b_i, stops when hitting another red phase, and waits for R_i until the beginning of the red phase.

This results is used to formulate the moving bottleneck cut as a renewal rewards process. The new bus cut, denoted by strategy s_3, is given by distribution $F_{s_3}(q)$ with mean μ_{s_3} and variance $\sigma^2_{s_3}$ obtained from eqs. 10. The new cut strategy is added to the set of strategies $s_3 \, \epsilon \, \Omega$ in eq. 11. Now, in order to solve the cut, μ_{s_3} and $\sigma^2_{s_3}$ are formulated below.

For a given renewal realization or "cycle" i, the distribution of the time elapsed T and the reward N need to be found. In this process, the reward is defined as the contribution to the cumulative count curve given by $N^i(B) + \Delta^i_{BP}$. In the equation, $N^i(B) = -x^i k$ is the contribution to the vehicle count at the boundary N_B and Δ^i_{BP} is contribution to the maximum number of vehicles crossed by the path Δ^i_{BP}. The time elapsed for each cycle is straightforward and is given by the sum of the running time, the dwell times, and red signal wait time. The reward is obtained by considering the running time L/v multiplied by the passing rate of a moving bottleneck $Q\left(\frac{n-1}{n}\right)\left(1/v - 1/w^\sharp\right)\big)$ and the dwell times S multiplied by the passing rate of a stationary bottleneck $Q\left(\frac{n-1}{n}\right)$. The values are formulated:

$$T_i = \frac{L_i}{v} + S_i + R_i \tag{37a}$$

$$N_i = L_i k + \frac{L_i}{v} Q\left(\frac{n-1}{n}\right)\left(1 - \frac{v}{w^\sharp}\right) + S_i Q\left(\frac{n-1}{n}\right) \tag{37b}$$

The mean, variance and covariance of the cycle time and reward are obtained directly (i subscript is dropped):

$$\mu_T = \mu_L/v + \mu_S + \mu_R, \tag{38a}$$

$$\mu_N = C_1\mu_L + C_2\mu_S, \tag{38b}$$

$$\sigma_T^2 = \sigma_L^2/v^2 + \sigma_S^2 + \frac{1}{v}Cov(L,S), \tag{38c}$$

$$\sigma_N^2 = C_1^2\sigma_L^2 + C_2\sigma_S^2 + 2C_1C_2Cov(L,S), \tag{38d}$$

$$Cov(T,N) = \sigma_L^2 C_1/v + \sigma_S^2 C_2. \tag{38e}$$

where $C_1 = Q\left(\frac{n-1}{n}\right)\left(1/v - 1/w^\sharp\right)$ and $C_2 = Q\left(\frac{n-1}{n}\right)$. Formulating the mean and the variance of L and R has already been accomplished on (33), where:

$$\mu_L = \mu_l\mu_n, \tag{39a}$$

$$\sigma_L^2 = \sigma_l^2\mu_n + \mu_l^2\sigma_n^2, \tag{39b}$$

$$\mu_R = \frac{1}{2}\mu_r(1+\delta^2), \tag{39c}$$

$$\sigma_R^2 = (\delta\mu_R)^2, \tag{39d}$$

where,

$$\mu_b = (\mu_r + \mu_g)/\mu_r, \tag{40a}$$

$$\sigma_b^2 = \mu_g(\mu_r + \mu_g)/\mu_r^2, \tag{40b}$$

There are still some variables that need to be formulated to solve eqs. 38 which are the mean, variance and covariance terms of S. Recall that S is the sum of dwell times for each street segment j:

$$S = \sum_j^n = D_j, \tag{41}$$

where D is the dwell time at each midblock and has been described on the previous section. The sum of dwell times S is thus dependent on n and D which are also random variables. By conditioning on n, the mean, variance and covariance terms of S can be obtained:

$$\mu_S = \mu_n \mu_D, \tag{42a}$$

$$\sigma_S^2 = \mu_D \sigma_n^2 + \mu_n \sigma_D^2, \tag{42b}$$

$$Cov(S, L) = \mu_D \mu_L \sigma_n^2. \tag{42c}$$

Recall from the last section that $\mu_D = \mu_d p_s$ and $\sigma_D^2 = p_s\left(\mu_d^2(1-p_s) + \sigma_d^2\right)$. Now, eqs. 38 can be solved by solving substituting for the mean, variance and covariance terms of D, S, L and R. However, the formulation is quite long and messy due to the large number of parameters. Therefore, the equation is reformulated with dimensionless parameters: $\rho = \mu_r/\mu_g$, $\lambda = \mu_l/\mu_g$, $\eta = (n-1)/n$, $\nu = v/w^\sharp$ and $\Delta = p_s\mu_d/\mu_g$. The ρ and λ parameters have been introduced already, but three new ones are presented. The variable η gives the percentage lane reduction , ν provides the bus free-flow speed normalized by the car free-flow speed and Δ gives the average dwell time per street segment normalized by the mean green time. Also, the canonical transformations from eqs. 12, 13 and 14 are applied to reduce the number of parameters. Eqs. 38 are reformulated:

$$\mu_T = \mu_g \frac{(1+\delta^2)\rho^2 + 2p_s\Delta(1+\rho) + \lambda(1+\rho)/\nu}{2\rho}, \tag{43a}$$

$$\mu_N = \mu_g \left(C_2 \Delta p_s + C_1 \lambda\right) \frac{1+\rho}{\rho}, \tag{43b}$$

$$\sigma_T^2 = f_1(\lambda, \rho, \eta, \nu, \Delta, p_s), \tag{43c}$$

$$\sigma_N^2 = f_2(\lambda, \rho, \eta, \nu, \Delta, p_s), \tag{43d}$$

$$Cov(T, N) = f_3(\lambda, \rho, \eta, \nu, \Delta, p_s), \tag{43e}$$

where $C_1 = \eta(1 - 1/\nu)/2$, $C_2 = \eta$ and f_1 and f_2 are long functions that are shown on Appendix A. Now, the cut distribution $F_{s_3}(q)$ is solved by using 5.2.3 to evaluate

the mean and variance values from eq. 10:

$$\mu_{s_3} = \frac{(1+\rho)(\eta\lambda + (2\Delta\eta + \lambda + 2k\lambda - \eta\lambda)\nu)}{\lambda(1+\rho) + 2\Delta\nu + \rho(2\Delta + \rho + \delta^2\rho)\nu} \tag{44a}$$

$$\sigma^2_{s_3} = \frac{\mu_g}{t} f(\lambda, \rho, \eta, \nu, \Delta) \tag{44b}$$

where $f(\lambda, \rho, \eta, \nu, \Delta)$ is a rather intractable function.

5.2.4 Short-block cut extension

In this paper, the short-block formulation is extended from a point estimate to a distribution. The prediction response variance of 0.02366 is obtained from the regression data set used in (33). By assuming that the variance is constant across all independent variables, one can build a distribution of the "short-block" cut with mean given in eq. 15. This new cut, $F_{s_4}(q)$ with routing strategy s_4, is incorporated into the MFD distribution by adding it to the set of strategies $s_5 \epsilon \Omega$ in eq. (11).

5.3 Results

In this section the multimodal corridor MFD model is compared with micro-simulation results. The simulation uses a cellular automaton model and gives the exact solution of the kinematic wave model with a triangular fundamental diagram, (12). Each simulation point corresponds to a stochastic corridor realization with defined λ, ρ and δ random variables. For each run, a randomized vehicle density is drawn from an uniform distribution between 0 and 1, while a bus proportion is drawn from 0 to 0.15. Each vehicle that is inserted into the corridor has a probability of being a bus given by the latter proportion. The bus flow q_b is obtained from the simulation and converted to an average headway $h = 1/(q_b n)$.

First, the comparison for one stochastic corridor is presented in fig. 20. Notice that in the figure, model results are given by the mean (red) and the 90% prediction band (blue) of the distribution. The latter is obtained by considering the area between the 5^{th} and the 95^{th} percentile curves of the distribution. The results show that:

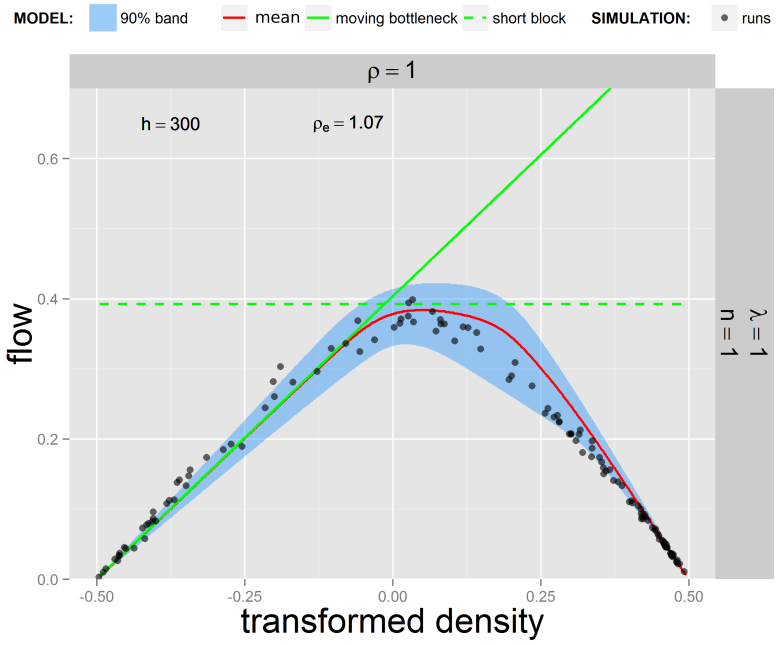

Figure 20: The multimodal corridor MFD model is compared to simulation results for one stochastic corridor given by $\lambda = 1$, $\rho = 1$, $\delta = 0.2$ and $n = 1$ lane. The triangular fundamental diagram input values are: $w^\sharp = 80$ km/h, $w^\flat = 20$ km/h, $Q = 2400$ veh/h . The bus operation parameters are: $w^\flat = 60$ km/h, $p_s = 1/3$, $d = 20$ s. The topology parameters are: $B = 15$ blocks, $\mu_g = 36$ s, time aggregation = 15 min, cell size = 6.67 m.

1) Simulation results fall within the 90% prediction band of the model.

2) The red/green effective ratio $\rho_e = 1.07$ is greater than the traffic signal ratio $\rho = 1.00$. This difference shows how much the red and green times are affected when considering the interactive effect of traffic signals and "bus signals"

3) The moving bottleneck cut captures the observed MFD asymmetry which is skewed to the right. This indicates that the moving bottleneck effect has a significant effect on the free-flow MFD region.

Now, more stochastic corridors are analyzed in order to verify that the model results are consistent with simulation results for a large range of inputs. The comparison is given in fig. 21 where each diagram represents a stochastic corridor with

varying parameters λ, ρ and headway. Notice that each diagram has a randomized headway in order to test for a wide variety of ranges. The figure provides the following insight:

1 The model provides a reasonable approximation to simulation results. The moving bottleneck cut and the short-block cut are essential when providing a tight approximation to the MFD.

2 The short-block cut has a large effect on corridors with $\lambda \leq 1.0$, and a smaller effect for the 1.5 value.

3 The MFD loses its symmetric property as the diagram is skewed to the right from the moving bottleneck effect. This effect shifts the optimal density where maximum flow is reached for some corridor cases.

4 The moving bottleneck effect has a larger effect for one-lane corridors compared to two-lane corridors. This is expected since vehicles can pass the bus on adjacent lanes when there is more than one lane.

5.4 Discussion

The main result of this chapter is that the existing corridor model can be extended to multimodal corridors with seven parameters λ,ρ,δ,η, ν, Δ and p_s. The moving bottleneck effect is formulated as a distribution in the context of MFD theory. Also, the bus short-block effect, which affects all cuts is incorporated by modifying the effective red/green ratio ρ_e.

Future work needs to focus on adding more realistic operations to the framework and seeing if and how they affect results. For instance, some variability in average bus speeds is incorporated with the p_s and d parameters. However, it is assumed that bus running speeds are deterministic at v, even though these speeds vary in

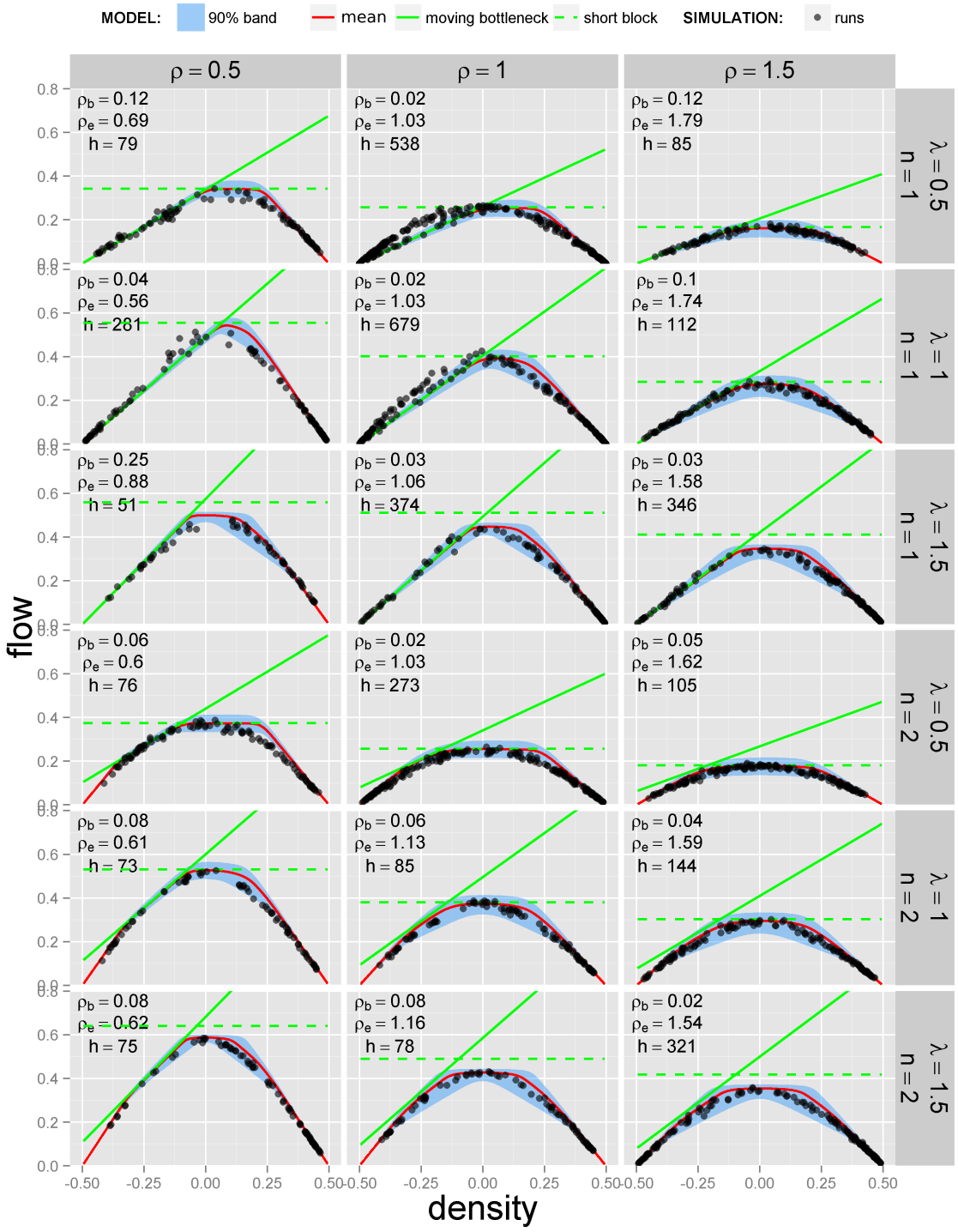

Figure 21: The multimodal corridor MFD model is compared to simulation results. The triangular fundamental diagram input values are: $w^\sharp = 80$ km/h, $w^\flat = 20$ km/h, $Q = 2400$ veh/h . The bus operation parameters are: $w^\flat = 60$ km/h, $p_s = 1/3$, $d = 20$ s. The topology parameters are: $B = 15$ blocks, $\mu_g = 36$ s, time aggregation = 15 min, cell size = 6.67 m.

real-life corridors. Analyzing if this variability greatly impacts the MFD is worthwhile. Furthermore, bus speeds are assumed to be free-flowing which gives a great approximation to the vehicular MFD. However, it is also important to evaluate how average bus speeds change with changing traffic conditions in the MFD.

Stochastic corridors assume no turns or routing. The next step is to study networks that can incorporate more realistic driving behavior.

CHAPTER VI

BUS EFFECTS ON STOCHASTIC NETWORKS

City roadway transportation systems are very complex since they have varying topological layouts, vehicle demands, path alternatives and flow capacities. Since the number of city structure configurations is endless, networks are approximated by a Manhattan grid pattern comprised of various stochastic ring-corridors. This allows for the extension of the corridor models for network operations.

6.1 Problem definition

The "stochastic network" random variable is defined as a square grid with $C = 4B$ stochastic ring-corridors spanning the four cardinal directions; see fig. 22. The number of corridors can be be broken down into $C/2$ "EW" corridors on the east-west and west-east directions and $C/2$ "NS" corridors on the north-south and south-north directions. Segment lengths, green times and red times are obtained from random variables l, g_{EW}, g_{NS}, r_{EW}, and r_{NS}. The variables are i.i.d. with mean $\mu_{\_}$, standard deviation $\sigma_{\_}$, and coefficient of variation (cov) parameters given by $\delta = \mu_{\_}/\sigma_{\_}$ where "_" is a placeholder for any of the random variables. It is assumed that the cov for all random variables are equal, $\delta = \delta_l = \delta_{g_{EW}} = \delta_{r_{EW}} = \delta_{g_{NS}} = \delta_{r_{NS}}$. Considering that a red signal on the EW corridors corresponds to a green signal on the NS direction and vice-versa, then $g_{EW} = r_{NS}$ and $g_{NS} = r_{EW}$. This corresponds to varying red/green ratios given by ρ_{EW} and $\rho_{NS} = 1/\rho_{EW}$ respectively. Also, since average green times vary for each direction, then each corridor type has a different dimensionless length value given by $\lambda_{EW} = l_{EW}/g_{EW}$ and $\lambda_{NS} = l_{NS}/g_{NS}$.

Vehicles on the corridor follow a triangular fundamental diagram, as defined by the kinematic wave (KW) theory of traffic (35; 44), with free-flow speed $w^\sharp$, congestion

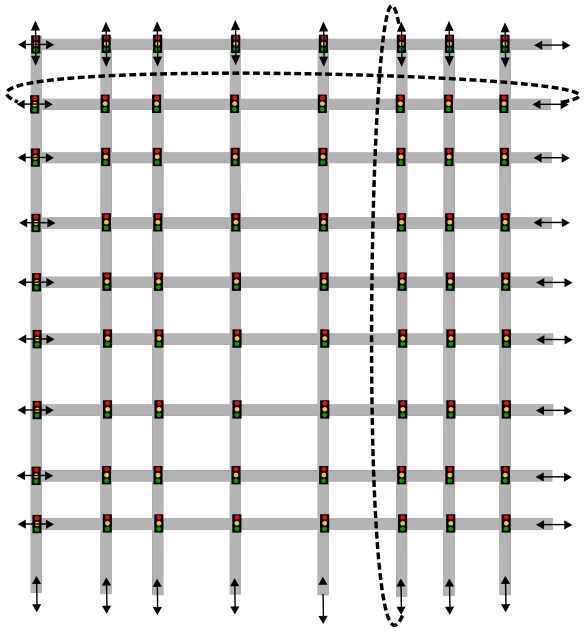

Figure 22: ring network

wave speed $-w^\flat$, jam density κ, and saturation flow $Q = \kappa w^\sharp w^\flat/(w^\sharp + w^\flat)$. The difference between a single corridor from a network and the "stochastic corridor" is that turns and routing are introduced. Therefore, traffic conditions from a corridor might affect conditions on another corridor. The O-D table is evenly spread across the network which ensures that demand is homogeneous across the network.

Buses travel on straight paths along the ring-corridors and do not make turns. Buses have a free-flow speed, v, probability of stopping at each block p_s, and a dwell time random variable d obtained from a normal distribution with μ_d and coefficient of variation δ. Buses do not operate on all corridors, but only on the ones where bus routes are defined. They operate on all lanes, but make stops on the outside lane. A bus that is not making a stop can pass another bus that is making a stop on the inside lane.

For each stochastic network realization a density k is defined and a proportion of buses k_b/k is chosen for the corridors that contain buses. Each vehicle on these corridors will then have a given probability of being a bus or a car based on this

proportion.

An analytical method to estimate the network MFD does not exist. Therefore, the first section of this chapter focuses on extending the corridor models to networks with one vehicle class. Then, the effect of buses is introduced on the subsequent section.

6.2 Network MFD model

This section focuses on combining ρ and λ values for each NS and EW corridor into effective values for the whole network. In order to aggregate the values, a weighted average is estimated based on the density on each corridor type. Then, the network can be evaluated as the aggregation of C corridors with effective parameters. The next subsection describes how a density proportion is derived and the subsequent subsection focuses on aggregating the inputs based on the density proportion.

6.2.1 Density proportion

Using Edie's generalized traffic flow equations (18) density for the two corridor types is given by $k_{EW} = T_{EW}/A_{EW}$ and $k_{NS} = T_{NS}/A_{NS}$. The variables T_{EW} and T_{NS} represent the total vehicle-time spent during a time aggregation period and A_{NS} and A_{EW} are the time-distance areas comprised of the time aggregation period multiplied by the network lane-length. The aggregation time period is the same for the whole network, and the length of EW and NS corridors are approximately equal for a large number of segments. Therefore, it is assumed that $A_{NS} \approx A_{EW}$ and the proportion of EW street density to the total density can be reformulated as:

$$\alpha = \frac{k_{EW}}{k_{EW} + k_{NS}} \approx \frac{T_{EW}}{T_{EW} + T_{NS}} \tag{45}$$

Finding the total vehicle-time spent on each corridor type is not a trivial task and depends on the levels of congestion on each corridor type. As an approximation, traffic conditions are assumed to be free-flowing which simplifies the total time spent

by vehicles on EW and NS streets as the total vehicle-distance covered by all vehicles divided by the free-flow speed:

$$\begin{aligned} T_{EW} &= D_{EW}/\omega^{\#}_{EW}, \\ T_{NS} &= D_{NS}/\omega^{\#}_{NS}. \end{aligned} \tag{46}$$

Where D_{EW} and D_{NS} are the total vehicle-distance for each corridor type while $\omega^{\#}_{EW}$ and $\omega^{\#}_{NS}$ are the free-flow average speeds. The next step is to find an approximation for the distance covered. First, consider a vehicle traveling from an origin to a destination with a Manhattan distance equal to $d = d_{EW} + d_{NS}$ where d_{EW} and d_{NS} are the distance on the EW and NS corridors respectively. If free-flow conditions are assumed, then the vehicle takes a shortest distance path since no traffic congestion is present and will travel a total distance of $d_{EW} + d_{NS}$. Now, since the O-D table is homogeneously distributed across the network, then for a random O-D pair the d_{EW} and d_{NS} random variables have an equal distribution. Therefore, the expected distance covered on each corridor type is approximately equal: $D_{EW} \approx D_{NS}$. This gives an approximation to eq. (45):

$$\alpha = \frac{1/w^{\#}_{EW}}{1/w^{\#}_{EW} + 1/w^{\#}_{NS}} \tag{47}$$

The next step is to evaluate the average free-flow speeds. This is done modeling a car trajectory as a renewal reward process that travels with free-flow speed $w^{\#}$ for a distance L_i, stops whenever it hits a red signal phase for duration R_i, and continues its trajectory at the end of the phase. The reward of the process is the distance covered L_i and the time elapsed is $T_i = L_i/w^{\sharp} + Ri$. Each renewal "cycle" starts and ends at the end of subsequent red phases encountered by the vehicle. Renewal reward theory states that the average free-flow speed is obtained as the expected value of the reward divided by the expected value of the time elapsed on each cycle (the i subscript is dropped):

$$w^{\#}_{\_} = \frac{\mu_{L\_}}{\mu_{T\_}} = \frac{\mu_{L\_}}{(\mu_{L\_}/w^{\#} + \mu_{R\_})} \tag{48}$$

where _ is a placeholder for each type of corridor and can take "EW' and "NS" values. Notice that the μ_L and μ_R values are different for each corridor type. Therefore, the average speed also differs:

$$w_{-}^{\#} = \frac{1}{1/w^{\#} + C_{-}} \quad \text{where } C_{-} = \frac{\rho_{-}^2(1+\delta^2)}{2(1+\rho_{-})\lambda_{-}} \tag{49}$$

Substituting these values on eq. 47 to reformulate α yields the following (long) equation:

$$\alpha = \frac{((1+\delta^2)w^{\sharp}\rho_{EW}^2 + 2\lambda_{EW}(1+\rho_{EW}))(1+\rho_{NS})}{4\lambda_{EW}(1+\rho_{EW})(1+\rho_{NS}) + (1+\delta^2)w^{\sharp}(\mu_{r_{NS}}/\mu_{g_{EW}}(1+\rho_{EW})\rho_{NS} + \rho_{EW}^2(1+\rho_{NS}))} \tag{50a}$$

Using the fact that a green signal on EW corridors translates to a red signal on NS and vice-versa, then $\rho_{EW} = 1/\rho_{NS}$ and $\mu_{r_{NS}} = \mu_{g_{EW}}$. This simplifies the equation:

$$\alpha = \frac{(1+\delta^2)w^{\sharp}\rho_{EW}^2 + 2\lambda_{EW}(1+\rho_{EW})}{4\lambda_{EW}(1+\rho_{EW}) + (1+\delta^2)w^{\sharp}(1+\rho_{EW}^2)} \tag{51}$$

Notice that only the parameters on the EW corridor type are necessary to estimate α. Also, remember that this is an approximation for free-flow conditions. On the simulation results this ratio is tested to see how it behaves during free-flow, near-capacity, and congested conditions.

6.2.2 Evaluating network effective inputs

An approximation method is presented which weights the ρ and λ parameters based on the density proportion given by α. Finding an effective dimensionless length is straightforward and is done as a simple weighted average:

$$\lambda_e = \alpha\lambda_{EW} + (1-\alpha)\lambda_{NS}, \tag{52}$$

where $\lambda_{EW} = \mu_l/\mu_{g_{EW}}$ and $\lambda_{NS} = \mu_l/\mu_{g_{NS}}$. Before finding an effective red/green ratio, effective red and green times are weighted by the density ratio:

$$\mu_{g_e} = \alpha\mu_{g_{EW}} + (1-\alpha)\mu_{g_{NS}}, \tag{53a}$$

$$\mu_{r_e} = \alpha\mu_{r_{EW}} + (1-\alpha)\mu_{r_{NS}}, \tag{53b}$$

where μ_{g_e} and μ_{r_e} are the effective expected red and green times . By dividing all terms by the expected cycle time μ_c which can take values $\mu_{g_{EW}} + \mu_{r_{EW}}$ or $\mu_{r_{NS}} + \mu_{r_{NS}}$, then eqs. 53 change to:

$$P_{g_e} = \alpha \frac{\rho_{EW}}{1 + \rho_{EW}} + (1 - \alpha) \frac{1}{1 + \rho_{EW}}, \tag{54a}$$

$$P_{r_e} = \alpha \frac{\rho_{NS}}{1 + \rho_{NS}} + (1 - \alpha) \frac{1}{1 + \rho_{NS}}, \tag{54b}$$

where P_{g_e} and P_{r_e} are the effective proportions of green and red time. Finally, the red/green ratio is obtained from these proportions:

$$\rho_e = P_{r_e}/P_{g_e} = \frac{\rho_{NS} + \rho_{NS}\rho_{EW} + \alpha(\rho_{EW} - \rho_{NS})}{1 + \rho_{EW} - \alpha(\rho_{EW} - \rho_{NS})} \tag{55}$$

By using the network property that $\rho_{NS} = 1/\rho_{EW}$ the ratio is simplified to:

$$\rho^e = \frac{1 + \alpha(\rho_{EW} - 1)}{\rho_{EW} - \alpha(\rho_{EW} - 1)}. \tag{56}$$

The effective values can now be applied to all corridors in the network.

The range of the effective value ρ^e is analyzed. By substituting for α from eq. 49 into eq. 56 ρ_{EW} can be reformulated as:

$$\rho^e = \frac{C_1(1 + \rho_{EW}) + C_2\rho_{EW}(\rho_{EW} + 1/\rho_{EW} - 1)}{C_1(1 + \rho_{EW}) + C_2\rho_{EW}}, \tag{57}$$

where $C_1 = 2\lambda_{EW}$ and $C_2 = (1 + \delta^2)w^{\#}$. Notice that if $\rho^{EW} = 1$, then $\rho^e = 1$ as expected, and if ρ^{EW} takes any other value, $\rho^e > 1$. This is a very interesting result that indicates that effective red times are always greater than effective green times whenever traffic parameters vary across the network.

6.2.3 No short-block effect?

It is not clear whether the short-block effect is present on real-life networks. This is because vehicles can turn from cross-streets into a street segment even when the upstream signal is red. Therefore, the loss in capacity from the upstream signal is mitigated from turning vehicles. However, if vehicles do not adapt around congestion

and into underutilized network space, then short-block effects might arise. In the simulation results on the next section, the model assumes that vehicles have high adaptability to traffic and therefore the short-block cut is omitted.

6.2.4 Numerical approximation to the network MFD

In this section, a numerical method is presented to approximate the network MFD by aggregating the flow and density of C corridors with effective parameters ρ_e and λ_e. The network MFD flow and density is obtained by a weighted average of all corridors (13):

$$Q(K) = \frac{\sum_{i=1}^{C} q_i(k_i) L_i}{\sum_{i=1}^{C} L_i}, \tag{58a}$$

$$K = \frac{\sum_{i=1}^{C} k_i L_i}{\sum_{i=1}^{C} L_i}, \tag{58b}$$

$$\tag{58c}$$

where Q is the network flow, K is the network density, q is the corridor flow and k is the corridor density for corridor i. The length of the corridor L is a random variable comprised of the lengths of all its street segments:

$$L = \sum_{j=1}^{B} l_j, \tag{59}$$

where l is the length of street segment j. Since l_j is assumed to be normal, then L has mean $B\mu_l$ and variance $B\sigma_l$. The flow equations are simplified by assuming that the network density is evenly distributed for the two corridor types, and thus EW and NS corridors have an equal density K. Notice that this is not realistic assumption for the real network with varying properties, but it is realistic for a homogeneously loaded network with effective parameters. Equation 58 becomes:

$$Q(K) = \frac{\sum_{i=1}^{C} q_i(K) * L_i}{\sum_{i=1}^{C} L_i}, \tag{60}$$

The distribution of eq. 60 does not have a closed form analytically, therefore, a Monte Carlo approach is used. For each value of K, 1000 network realization are

simulated. For each realization $q_i(K)$ is randomly drawn C times from the corridor MFD model and two length values L_j are randomly drawn for EW and NS each. Then, eq. 60 is used to estimate one network flow value $Q(K)$ for a given realization of a network. The network MFD distribution is obtained from the simulated points.

6.2.5 Simulation assignment

Vehicles begin and end their trajectories at predetermined intersections. In order to conserve a constant density, a vehicle is reinserted into the network at the same time that another vehicle exits the network. The origin-destination (OD) demand is evenly distributed across the network such that the newly inserted vehicle has an equal probability of being matched with any available OD pair.

Routing between two points is performed by a series of steps. First, the maximum number of independent shortest distance paths is obtained. Notice that for a Manhattan grid, each intersection pair will have four independent paths which helps to reduce the number of paths that need to be evaluated. The next step is to assign weights to each path based on different routing strategies, which are described on the next paragraph. Finally using these weights, logit probabilities are estimated for each path, and one of the paths is chosen from a random draw based on the probabilities. The β coefficient for the logit function is defined as $1/(w_{max} - w_{min})$, where w_{max} and w_{min} are the maximum and minimum weights from the set of independent paths.

Three different routing strategies are tested with increasing levels of adaptability to congestion. Each one has a different way to assign link weights:

- Strategy 1: Routing is defined by shortest Manhattan distance and vehicles choose a route right before they start their trip. Weights are defined by segment length.

- Strategy 2: Routing is defined by shortest travel time and vehicles choose a route right before the start of their trip. If a vehicle exiting a street segment is

stuck for more than 5 seconds, then it re-routes. Weights are defined by segment travel time.

- Strategy 3: Routing is defined by shortest travel time and vehicles re-route at every intersection encountered. Weights are defined by segment travel time.

6.2.6 Results

In this section the network MFD model is compared to simulation results from the cellular automaton model in Appendix A. The simulation consists of $B = 10$ blocks and $C = 40$ corridors. For a simulation run, only λ, ρ_{EW}, and δ need to be defined. Notice that ρ_{NS} is be the reciprocal of ρ_{EW} and does not need to be specified. For each run, the network topography is defined by randomly drawing B segment lengths for EW corridors and B segment lengths for NS corridors. Signal parameters vary across time and distance with a specified ρ_{st} and cycle length. Finally, for each run, a randomized vehicle density between 0 and 1 is drawn.

Before showing results for a wide range of stochastic networks, one network is analyzed in fig. 23. The results provides the following insight:

1) Strategy 1 performs poorly compared to other strategies. This is expected because vehicles are not able to re-route based on traffic conditions. The MFD loses its symmetric property during the congested region as flow drops precipitously to a break down. This suggests that traffic gridlock occurs as vehicles cannot re-route to find better routes.

2) Strategy 2 performs marginally better than strategy 1 as vehicles can choose their routes based on traffic conditions. Free-flow conditions are similar to strategy 1 and capacity conditions improve marginally. More importantly, during congested regions, flow is much higher and traffic gridlock is avoided as vehicles re-route when they get stuck.

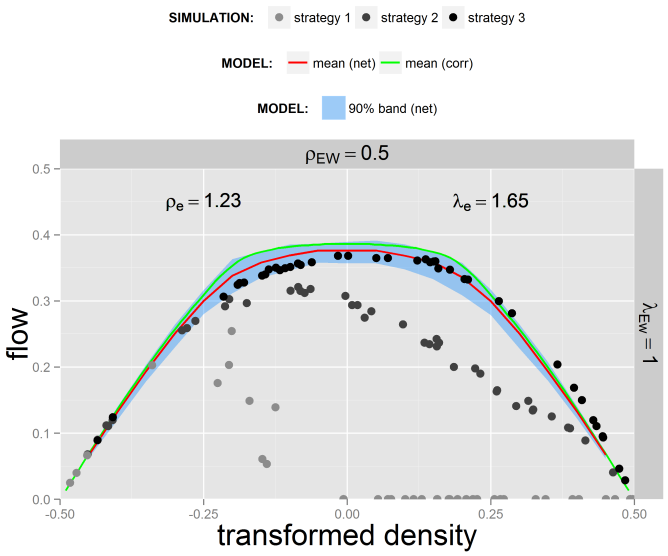

Figure 23: Comparison of model to simulation results of one network with parameters $\lambda_{EW} = 1.0$ and $\rho_{EW} = 0.5$. The triangular fundamental diagram input values are: $w^\sharp = 80$ km/h, $w^\flat = 20$ km/h, $Q = 2400$ veh/h . The bus operation parameters are: $w^\flat = 60$ km/h, $p_s = 1/3$, $d = 20$ s. The topology parameters are: $B = 10$ blocks, $n = 1$ lane, $\mu_g = 36$ s, time aggregation = 15 min, cell size = 7.5 m

3) Strategy 3, which provides the most adaptability to congestion, provides the highest flow and approximates the multimodal corridor MFD model. This result suggests that high routing adaptability is essential to reach full network capacity. Also, this indicates that the effective ρ_e, λ_e values provide a reasonable approximation to the capacity of the MFD.

4) The short-block cut is not active for strategy 3 as the model does not include this effect.

5) The median MFD curve for the corridor model with ρ_e, λ_e provides a very accurate approximation to the simulation results from strategy 3. This is an important result which indicates that the mean MFD curve can be obtained by evaluating the corridor MFD model at mean values λ_e, ρ_e and K (mean density).

The same analysis is performed on 8 additional stochastic networks in fig. 24. The results agree with the insight that is described above and can be generalized to a wide range of inputs.

The next step is to evaluate how the density proportion α between NS and EW corridors behaves during varying traffic conditions. The estimated value, on eq. 49, is compared to the actual value from simulated runs using routing strategy r_3. Determining the behavior of this parameter is important because it is used to determine the effective inputs that are used for the network model. The comparison between estimated and the actual α values is found on fig. 25. The results indicate that:

1) When ρ_{st} is equal to one, the estimated α value is 0.5 and the simulated value hovers around the estimate. This is expected since average red and green times are equal on EW and NS corridors. Therefore, average speeds are expected to be the similar and densities are expected to be evenly distributed along the network.

2) When ρ_{st} is not equal to one, the simulated α value varies depending on the network density. During near-capacity regions the value sometimes deviates from the estimate. During congested traffic, the value approaches 0.5 as it nears jam density.

3) The estimated α value is a great approximation during periods of light density, as expected. However, for some cases, the simulated value deviates from the estimate as congestion increases. Even as these parameters vary, the estimated α is sufficient to provide a reasonable MFD approximation as has already been observed on fig. 24

The next step is to examine the stability of travel times on the network with routing strategy r_3. 10 network simulation runs are performed on a large network with $B = 30$ blocks. Notice that the network size is increased for this experiment

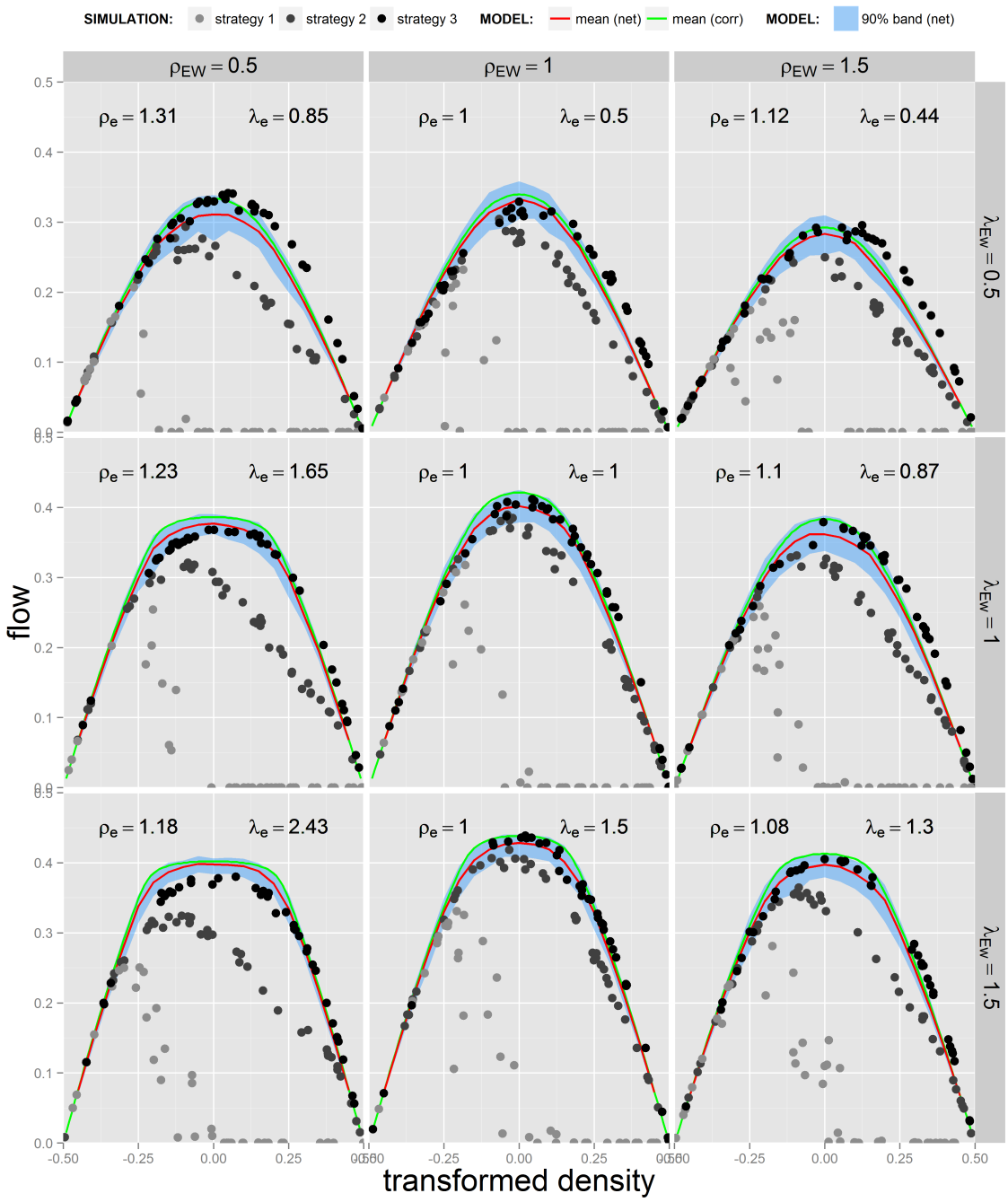

Figure 24: Comparison of model to simulation results of 9 different stochastic networks. The triangular fundamental diagram input values are: $w^\sharp = 80$ km/h, $w^\flat = 20$ km/h, $Q = 2400$ veh/h . The bus operation parameters are: $w^\flat = 60$ km/h, $p_s = 1/3$, $d = 20$ s. The topology parameters are: $B = 10$ blocks, $n = 1$ lane, $\mu_g = 36$ s, time aggregation $= 15$ min, cell size $= 7.5$ m

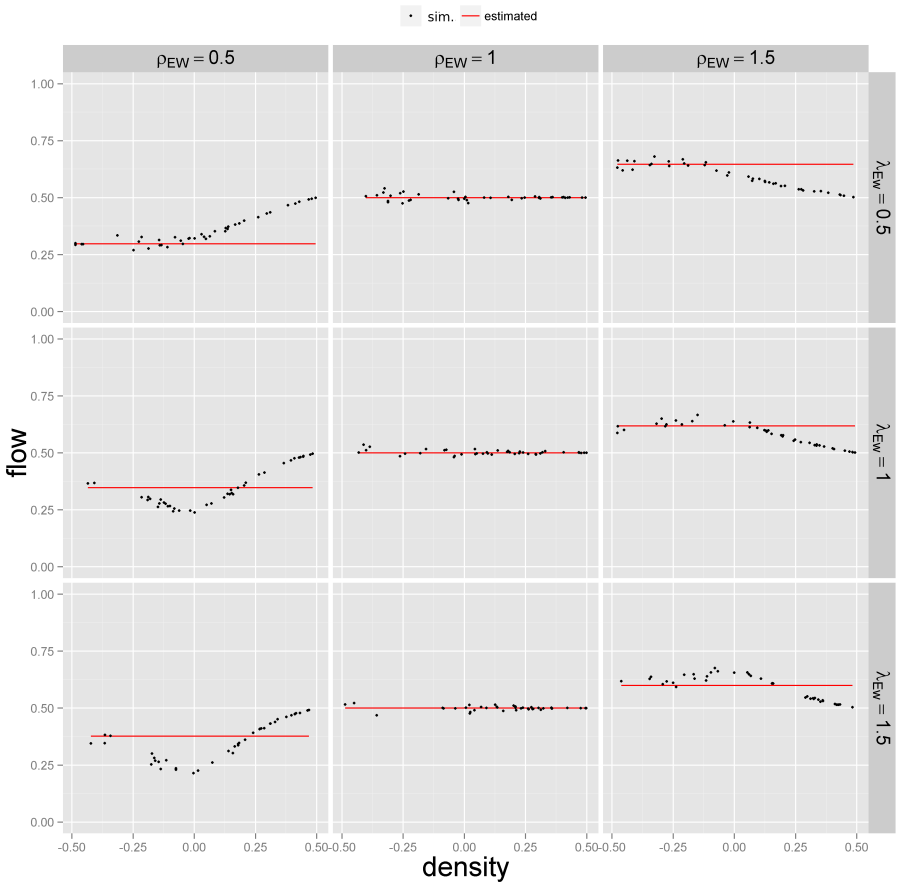

Figure 25: Comparison of the estimated approximation of α to values from the simulation. Same parameters are used as fig. 24

to obtain longer trips, which can now span a maximum of 15 blocks. In order to obtain a larger pool of trips for each O-D pair, the network is divided into regions of 2×2 blocks. Therefore, the O-D table covers 15×15 different regions. Ten different networks are run for an aggregation period of 15 minutes and vehicle travel times are grouped into bins for each O-D pair and time aggregation period. The travel time cov is estimated for all trips on each bin and the average Manhattan distance is estimated between the origin and destination. The bins with less than 10 vehicles trips recorded are discarded since they provide a small sample size. The results, which plot the average O-D Manhattan distance vs. the travel time cov is found on fig. 26. The results indicate that:

- There is a decreasing relationship between trip distance of an OD pair and the coefficient of variation. This likely occurs because travel times for short paths are very sensitive to variations in traffic signal delay and queue delay.
- The number of O-D pairs that have a stable travel time, where stability is defined as $cov < 0.3$, is 60%. However, if only paths larger than 10 or 15 street segments are considered, the number increases to 80% and 90% , respectively.
- Stochastic user equilibirum (SUE) holds for long trips as vehicles take minimum paths which have stable travel times.

6.3 Multimodal network MFD model

In order to account for bus operations, the bus short-block effect and the moving bottleneck effect from corridor models are extended to networks.

6.3.1 Bus short-block effect

Recall that the short-block effect is estimated by modeling buses as signalized intersections which are denoted as "bus signals". The capacity of an intersection is

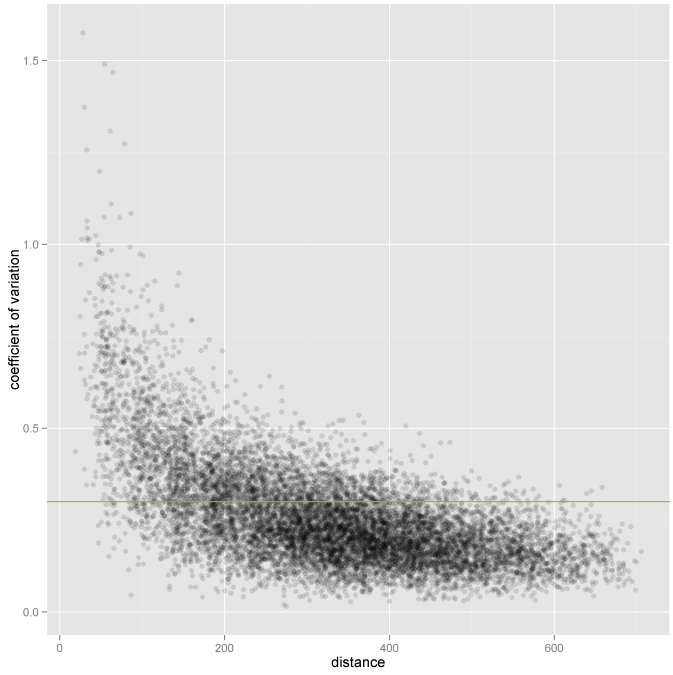

Figure 26: Evaluation of the coefficient of variation (cov) of travel times for O-D pairs during 15 min bins. Same parameters are used as fig. 24 except that $B = 30$ blocks

thus reduced by considering the combination of the bus signal and the existing traffic signal which is captured by an effective ρ value. In this subsection, an effective ρ is estimated for each corridor type EW and NS which are then aggregated into an effective ρ value for the whole network.

Buses do not operate on all roads but on routes where there is a large passenger demand. Therefore, the network consists of a mixture of corridors with buses and corridors without buses. In order to incorporate bus operations into the network model, some extensions are made. The first one deals with the reduction in intersection capacity from bus operations for EW and NS corridors separately. This method takes into account both corridor with buses and corridors without buses and combines them to obtain an effective red/green ratio for each corridor type ρ^e_{EW}, ρ^e_{EW}. Notice that changing these values causes the network relationship $\rho^e_{EW} = 1/\rho^e_{NS}$ to no longer hold for effective values.

For the set of EW (and NS) corridors, there are C_b multimodal corridors and $C_{nb} = C/2 - C_b$ car-only corridors. For the corridors with buses, it is assumed that only one lane includes bus operations, which is called the mixed lane. This assumption has proven to be reasonable for stochastic corridors. Therefore, multimodal corridors are comprised of 1 mixed-lane and $n-1$ car-only lanes while car-only corridors have n car-only lanes. Therefore the proportion of lanes to mixed lanes on NS and EW corridors is given by $n_e = C/2C_b$.

In order to model this behavior, concepts from the multimodal corridor MFD model are implemented. In equation 36 the effective red/green ratio is weighted based on $n-1$ car-only lanes and one mixed lane. Here, the ratio is obtained using the same concepts but considers $n_e - 1$ lanes without buses and one lane with buses. By applying eq. 36 for NS and EW corridors the following formulation is obtained:

$$\rho^e_{EW} = \rho_{EW} + \frac{\bar{\rho}_{EW}}{n^e_{EW}} + \frac{\rho_{EW}\bar{\rho}_{EW}}{n^e_{EW}}, \tag{61a}$$

$$\rho^e_{NS} = \rho_{NS} + \frac{\bar{\rho}_{NS}}{n^e_{NS}} + \frac{\rho_{NS}\bar{\rho}_{NS}}{n^e_{NS}}, \tag{61b}$$

where ρ^e_{EW} and ρ^e_{NS} are the effective ratios for each direction after accounting for bus operations, ρ_{EW} and ρ_{NS} are the values for the traffic signals and $\bar{\rho}_{EW}$ and $\bar{\rho}_{NS}$ are the parameters for the bus signals. The weighted average for the whole network is estimated using the density proportion from eqs. 52 and 57:

$$\rho^e = \frac{\rho^e_{EW} + \rho^e_{NS}\rho^e_{EW} + \alpha(\rho^e_{EW} - \rho^e_{NS})}{1 + \rho^e_{EW} - \alpha(\rho^e_{EW} - \rho^e_{NS})} \tag{62a}$$

$$\lambda^e = \lambda_{EW}\alpha + \lambda_{NS}(1-\alpha) \tag{62b}$$

6.3.2 Moving bottleneck effect

The moving bottleneck effect is expected to be small for networks since the number of lanes per mixed lane n_e is usually large compared to corridors. Regardless, this effect is evaluated in this section. Consider that the moving bottleneck effect varies for EW and NS corridors since each corridor has different signal parameters. Aggregating the

effects of each type into one cut seems to be a difficult task. Therefore, a simplification is made where effective parameters ρ^e, λ^e and n_e are used to solve the cut equations on eqs. 5.2.3. This assumes that the moving bottleneck effect which changes by corridor type, can be captured by solving a cut for a corridor with effective values.

6.3.3 Results

In this section a comparison between simulation results and the model is made. Each simulation point corresponds to a network realization with $B = 10$. Each street and avenue corridor is comprised of 2 lanes and 10 segment lengths that are drawn from the distribution of l. Buses operate on every other corridor, which gives a ratio of total lanes to bus-lanes of $n_e = 4$. For each run, a randomized density is chosen between 0 and 1, and vehicles are randomly spread out across the network. A randomized proportion of buses is chosen between 0 and 0.15. Each vehicle inserted into the network will have a probability of being bus according to the defined bus proportion. The bus flow q_b is obtained from the simulation and converted to an average headway $h = q_b * n$. The results, on fig. 27 indicates that the model provides a good approximation to the simulation. This indicates that:

- The effective λ and ρ and n values provide reasonable inputs to the simulation
- The short-block effect is not present for routing strategy r_3 where vehicles have full adaptability to congestion
- This case is only slightly different than the "no bus" case, which is likely attributed to the small proportion of mixed lanes $1/n_e = 1/4$. More interesting cases need to be analyzed where the proportion of mixed lanes is higher in order to evaluate how results are affected.

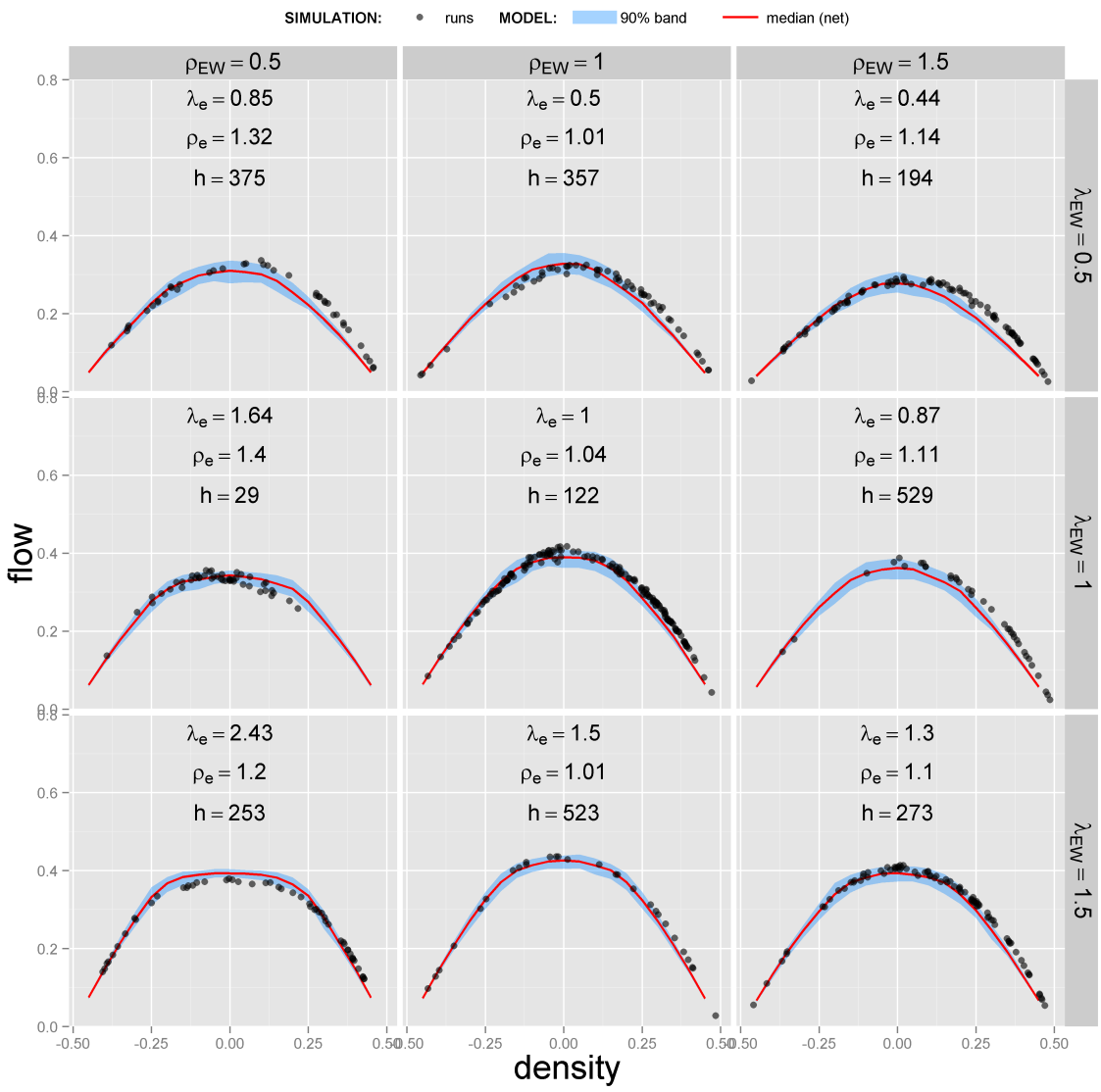

Figure 27: Comparison of model to simulation results of a multimodal network. The triangular fundamental diagram input values are: $w^\sharp = 80$ km/h, $w^\flat = 20$ km/h, $Q = 2400$ veh/h . The bus operation parameters are: $w^\flat = 60$ km/h, $p_s = 1/3$, $d = 20$ s. The topology parameters are: $B = 10$ blocks, $C = 40$ corridors, $C_b = 20$ corridors (every other corridor), $n = 2$ lanes, $\mu_g = 36$ s, time aggregation = 15 min, cell size = 7.5 m

6.4 Discussion

The main result of this paper is that multimodal networks can be modeled using only three parameters λ^e, ρ^e and δ. also, it provides a few extensions to the Corridor MFD Model which are interesting and practical. The first extension is the Network MFD Model to approximate the network MFD by considering the proportion of density on each corridor type. An analytical approximation method to evaluate the density proportion is presented by assuming free-flow conditions. Interestingly, the method suggests that effective ρ_e values are always larger than 1 when ρ values differ between each corridor type. This indicates that by having heterogeneous signalization parameters throughout the network, intersection capacity decreases.

One of the assumptions of this study is that the O-D table is homogeneously distributed along the network. In real-life networks, roads that have a large demand usually have a higher green/cycle ratio. Therefore, heterogeneity in the network demand along with heterogeneity in signalization parameters needs to be evaluated further. Finally, routing analysis shows that a network can achieve its full capacity if vehicles have full adaptability to congestion , otherwise the flow is reduced and congestion breakdown can occur. Adapting the network model to vehicles that do not have full adaptability can be a worthwhile investigation.

A limitation of the Multimodal MFD Corridor is that buses travel on straight paths along each corridor. In real-life networks buses often make turns and travel in only a few segments of the corridor. Therefore, each street segment has varying density in terms of bus proportions, which needs to be studied further. Finally, there is a need to verify the models with real-life data which is difficult to gather with current technology but will likely be attainable as data becomes more available.

CHAPTER VII

DISCUSSION

7.1 Contributions

This dissertation advances knowledge and understanding in multimodal urban mobility by developing parsimonious analytical models. These require only a few dimensionless parameters and do not have to be re-calibrated for different corridors or networks. The analytical approach is useful as it provide generalized results and provides insight into the problem. Current MFD theory focuses on corridor models with one vehicle class (cars). These are extended to account for bus operations and network systems.

For corridors, the moving bottleneck effect is formulated in the context of existing MFD theory requiring seven parameters. Also, the short-block bus effect is introduced to capture the complex interactions between buses and signalized intersections. This effect reduces the flow of the corridor MFD model by altering minimum paths on the variational theory time-space diagram. Modeling buses as stationary bottlenecks at downstream intersections is a straightforward way to approximate these effects. The short-block bus effect only requires three parameters evaluated at mean values: λ, ρ_e, and δ.

The network MFD with one vehicle class (cars) is formulated with only three dimensionless parameters: λ_e, ρ_e and δ. This model is estimated by considering the density proportion of vehicles on EW and NS corridors. Input parameters on each corridor type are then weighted based on this proportion to obtain effective parameters λ_e and ρ_e. An interesting result is that the effective red/green ratio parameter is always greater than one ($\rho_e > 1$) if signalization green and red parameters vary on

each corridor type. Additionally, simulation results suggest that full information and routing adaptability is necessary to reach the full capacity predicted by the network model.

Multimodal networks are solved by combining corridor bus effects and network effects from varying corridor properties. The models provide a reasonable approximation to simulation results when the proportion of mixed lanes is low at 1/4. Further analysis is necessary to evaluate networks with a higher proportion of mixed lanes.

7.2 Limitations

The models assume long corridors or ring corridors in order to maintain consistency with variational theory. However, as shown on this study, boundary effects on short corridors can influence the capacity of the MFD. These effects need to be evaluated further.

Bus operations are assumed to have instantaneous acceleration, i.i.d. dwell times, and mid-block stops. These assumptions are not realistic compared to real-life bus trajectories which have more intricate operations. However, the bus short-block effect and the moving bottleneck effect on corridors can be extended to evaluate complex bus trajectories, since these only require the mean running time spent between intersections. Also, it is assumed that buses operate on straight paths and have similar headways on multimodal corridors. In reality, bus routes include many turns and varying demand on each corridor.

Networks are assumed to have a Manhattan grid network structure with evenly distributed O-D demand. However, real-life networks have different topological structures and heterogeneous demand patterns, and it is unclear how these will affect the MFD. Furthermore, models assume that cars have full driver information and routing adaptability which is not the case in real-life operations. The effect of having less than perfect information degrades the capacity of a network as shown on previous

results.

The models do not account for more intricate traffic operations like left-turn operations, yellow and all-red signal phases, actuated traffic signals, and others. These operations are ignored in order to isolate bus effects, which is the purpose of the project. MFD models that can capture more realistic traffic operations needs to be evaluated further.

7.3 Future work

The models only address vehicle throughput, but person throughput is not considered. However, a simple experiment is performed to show how the models can be extended to include passengers on fig. 28. First, the relationship between dwell times and average bus passengers is established as in Boyaci & Geroliminis (5). The mean dwell time is assumed to be proportional to the average number of passengers on buses p_b by the following relationship $p_b = (\mu_d - 5sec)\phi$. Also, an average headway μ_h is defined, which by definition gives the average bus flow $q_b = 1/n\mu_h$. Finally, the average number of car passenger p_c are defined. By running the network model for $\lambda_e = 1.0$, $\rho_e = 1.0$, and $n_e = 2$, and varying the dwell times, the median line for the MFD line is found. Then, for each flow value q the car flow is obtained from $q_c = q - q_b$. Finally, the passenger capacity is obtained from $q_p = p_b q_b + p_c q_c$. In the figure, various vehicle and passenger MFDs are plotted for varying dwell times. Notice that different ϕs will result in vary different passenger MFD shapes. For instance, notice that for $\phi = 0.2$, the flow is monotonically increasing with varying dwell times, while for $\phi = 0.2$ this is not always the case. Also, notice that the critical vehicle density to maximize passenger flow varies for each curve. These are some examples of interesting results that can be derived from the model.

There are many potential areas to expand this work. First, a more in-depth person throughput needs to be considered to get a holistic view of multimodal networks.

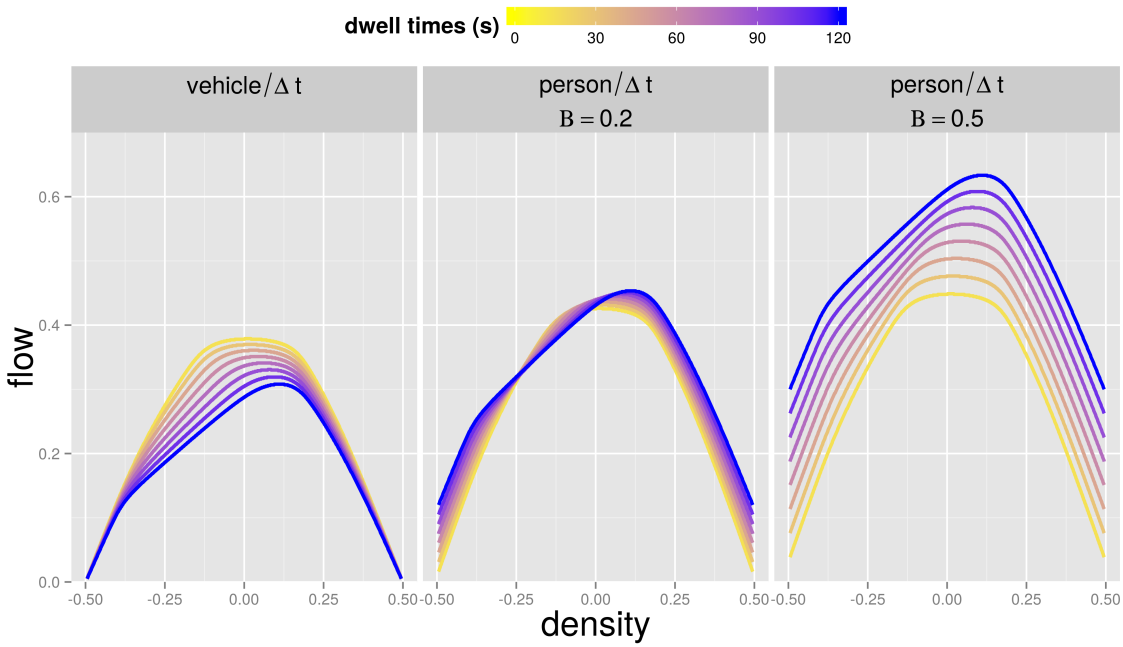

Figure 28: Person throughput analysis. The triangular fundamental diagram input values are: $w^\sharp = 80$ km/h, $w^\flat = 20$ km/h, $Q = 2400$ veh/h . The bus operation parameters are: $w^\flat = 60$ km/h, $p_s = 1/3$, $d = 20$ s. The topology parameters are: $B = 10$ blocks, $C = 40$ corridors, $C_b = 20$ corridors (every other corridor), $n = 2$ lanes, $\mu_g = 36$ s, time aggregation = 15 min, cell size = 7.5 m

This is a difficult task that likely requires mode-choice analysis. This greatly increases the complexity of the models as new parameters capturing people attitudes and preferences are introduced. Furthermore, more dynamic bus operations can be implemented. For instance, dwell times can be adjusted in correspondence to the board/alight demand at bus stops. Also, bus bunching is essential when determining the performance of the system and the wait time of passengers. These extensions can be applied to the model.

Also, one of the major benefits of the MFD approach is the ability to capture aggregate behavior from different signal and topological parameters. Therefore, there is a potential to extend analytical models for control strategies. For instance, the effect of transit signal priority, bus bunching control, bus-only lanes can be modeled.

Finally, an important future area of research is to come up with a simpler formulation for the stochastic models. Currently, equations are intractable and need to be solved numerically. However, curve fitting methods using the input parameters λ, ρ, δ, can provide a simple equation to estimate the MFD curves. This is essential as practitioners are more willing to apply and use a simple formulation.

7.4 Broader Impacts

The models account for the effects of bus operations, but can be extended to other type of slow-moving vehicles operating in mixed traffic. These can include trolleys, streetcars, bicycles, trucks, motorcycles and taxis. The operations of these modes differ greatly from buses but also exhibit slow running speeds and/or frequent stops. What's more, transit vehicles are not the only traffic disruption on urban networks. The models can be extended to include left-turns, delivery trucks, illegally parked vehicles, pedestrian crossings, and other effects.

As an example, left-turn operations can be modeled as stationary bottlenecks similar to the bus short-block effect. The bottleneck durations are going to be determined

by the time that a car waits for an acceptable turning gap while blocking one lane. Then, the effective red/green ratio ρ_e can be estimated to include the interactive effects between traffic signals and the left-turn operations. The stochastic corridor model is now evaluated with the new effective parameter. This example shows how the models can be easily extended to consider other traffic disruptions.

This project can have a significant impact on urban transportation planning. Understanding the cause and effect mechanisms of bus operations (and other types of traffic disruptions) on capacity can help to develop more accurate traffic models. Also, the application of these models is simple as it only requires a few parameters. This can lead to better informed decisions to alleviate congestion on multimodal traffic.

7.5 Acknowledgements

This research was supported by NSF research project 1301057.

APPENDIX A

EQUATIONS FOR MOVING BOTTLENECK CUT

$$f1 = \mu_g^2 \frac{1+\rho}{\rho^2}(-(\Delta C_2 p_s + C_1\lambda)^2 + (\Delta^2 C_2^2 p_s(-1+p_s-\delta^2) - C_1^2\delta^2\lambda^2)\rho)), \tag{63a}$$

$$f2 = \frac{1}{4\rho^2\nu^2}\mu_g^2(\lambda^2(1+\rho)(1+\delta^2\rho) + 2\Delta p_s\lambda(1+\rho)\nu + ((\delta+\delta^3)^2\rho^4 - 4\Delta^2 p_s(1+\rho)(p_s(-1+\rho) - (1+\delta^2)\rho))\nu^2), \tag{63b}$$

$$f3 = \frac{1}{2\rho^2\nu}(1+\rho)(\lambda(\Delta C_2 p_s + C1\lambda(1+\delta^2\rho)) + 2\Delta p_s(C1\lambda + \Delta C_2(p_s+\rho-p_s\rho+\delta^2\rho))\nu) \tag{63c}$$

Bibliography

[1] "Travel Model Validation and Reasonableness Checking Manual, Second Edition," tech. rep., Cambridge Sytematics, Inc., Federal Highway Administration, Cambridge, Massachusetts, 2010.

[2] Aboudolas, K. and Geroliminis, N., "Perimeter and boundary flow control in multi-reservoir heterogeneous networks," *Transportation Research Part B: Methodological*, vol. 55, pp. 265–281, 2013.

[3] Ardekani, S. and Herman, R., "Urban network-wide traffic variables and their relations," *Transportation Science*, vol. 21, no. 1, pp. 1–16, 1987.

[4] Bank, W., "World Bank," 2014.

[5] Boyaci, B. and Geroliminis, N., "Estimation of the Network Capacity for Multimodal Urban Systems," *Procedia - Social and Behavioral Sciences*, vol. 16, pp. 803–813, Jan. 2011.

[6] Buisson, C. and Ladier, C., "Exploring the Impact of Homogeneity of Traffic Measurements on the Existence of Macroscopic Fundamental Diagrams," *Transportation Research Record: Journal of the Transportation Research Board*, vol. 2124, pp. 127–136, Dec. 2009.

[7] Cassidy, M. J., "Bivariate relations in nearly stationary highway traffic," *Transportation Research Part B: Methodological*, vol. 32, no. 1, pp. 49–59, 1998.

[8] Cassidy, M. J. and Bertini, R. L., "Some traffic features at freeway bottlenecks," *Transportation Research Part B: Methodological*, vol. 33, no. 1, pp. 25–42, 1999.

[9] Daganzo, C. F., "Queue Spillovers in Transportation Networks with a Route Choice," *Transportation Science*, vol. 32, no. 1, pp. 3–11, 1998.

[10] Daganzo, C. F., "A variational formulation of kinematic waves: basic theory and complex boundary conditions," *Transportation Research Part B: Methodological*, vol. 39, pp. 187–196, Feb. 2005.

[11] Daganzo, C. F., "A variational formulation of kinematic waves: Solution methods," *Transportation Research Part B: Methodological*, vol. 39, pp. 934–950, Dec. 2005.

[12] Daganzo, C. F., "In traffic flow, cellular automata=kinematic waves," *Transportation Research Part B: Methodological*, vol. 40, pp. 396–403, June 2006.

[13] Daganzo, C. F., "Urban gridlock: Macroscopic modeling and mitigation approaches," *Transportation Research Part B: Methodological*, vol. 41, pp. 49–62, Jan. 2007.

[14] Daganzo, C. F., Gayah, V. V., and Gonzales, E. J., "Macroscopic relations of urban traffic variables: Bifurcations, multivaluedness and instability," *Transportation Research Part B: Methodological*, vol. 45, pp. 278–288, Jan. 2011.

[15] Daganzo, C. F. and Geroliminis, N., "An analytical approximation for the macroscopic fundamental diagram of urban traffic," *Transportation Research Part B: Methodological*, vol. 42, pp. 771–781, Nov. 2008.

[16] Daganzo, C. F. and Laval, J. a., "On the numerical treatment of moving bottlenecks," *Transportation Research Part B: Methodological*, vol. 39, pp. 31–46, Jan. 2005.

[17] Eberhard Hopf, "On the right weak solution of the cauchy problem for a quasilinear equation of first order," *Journal of Mathematics and Mechanics*, no. 19, pp. 483–487, 1970.

[18] Edie, L., "Discussion on Traffic Stream Measurements and Definitions," in *The 2nd International Symposium on the Theory of Traffic Flow*, 1963.

[19] Eichler, M. and Daganzo, C. F., "Bus lanes with intermittent priority: Strategy formulae and an evaluation," *Transportation Research Part B: Methodological*, vol. 40, pp. 731–744, Nov. 2006.

[20] El-Geneidy, A., Horning, J., and Krizek, K., "Analyzing Transit Service Reliability Using Detailed Data From Automatic Vehicular Locator Systems," *Journal of Advanced Transportation*, vol. 45, no. July 2010, pp. 66–79, 2011.

[21] Evans, L., *Partial Differential Equations*. American Mathematical Society, 2 ed., 2010.

[22] Gayah, V. V. and Daganzo, C. F., "Effects of Turning Maneuvers and Route Choice on a Simple Network," *Transportation Research Record: Journal of the Transportation Research Board*, vol. 2249, pp. 15–19, Dec. 2011.

[23] Gazis, D. and Herman, R., "The Moving and "Phantom" Bottlenecks," *Transportation Science*, 1992.

[24] Geroliminis, N. and Boyac, B., "The effect of variability of urban systems characteristics in the network capacity," *Transportation Research Part B: Methodological*, vol. 46, pp. 1607–1623, Dec. 2012.

[25] Geroliminis, N. and Daganzo, C. F., "Macroscopic modeling of traffic in cities," *TRB 86th Annual Meeting*, no. January, 2007.

[26] Geroliminis, N. and Daganzo, C. F., "Existence of urban-scale macroscopic fundamental diagrams: Some experimental findings," *Transportation Research Part B: Methodological*, vol. 42, pp. 759–770, Nov. 2008.

[27] Geroliminis, N., Zheng, N., and Ampountolas, K., "A three-dimensional macroscopic fundamental diagram for mixed bi-modal urban networks," *Transportation Research Part C: Emerging Technologies*, vol. 42, pp. 168–181, May 2014.

[28] Godfrey, J. W., "The Mechanism or a Road Network," *Traffic Engineering and Control*, vol. 11, no. 7, pp. 323–327, 1969.

[29] Gonzales, E., Chavis, C., Li, Y., and Daganzo, C., "Multimodal Transport in Nairobi , Kenya : Insights and Recommendations with a Macroscopic Evidence-Based Model," in *TRB 86th Annual Meeting , Compendium of papers CD-ROM*, pp. 1–17, 2011.

[30] Gonzales, E. J. and Daganzo, C. F., "Morning commute with competing modes and distributed demand: User equilibrium, system optimum, and pricing," *Transportation Research Part B: Methodological*, vol. 46, no. 10, pp. 1519–1534, 2012.

[31] Ji, Y. and Geroliminis, N., "On the spatial partitioning of urban transportation networks," *Transportation Research Part B: Methodological*, vol. 46, no. 10, pp. 1639–1656, 2012.

[32] Koshy, R. Z. and Arasan, V. T., "Influence of Bus Stops on Flow Characteristics of Mixed Traffic," *Journal of Transportation Engineering*, vol. 131, no. 8, pp. 640–643, 2005.

[33] Laval, J. A. and Castrillon, F., "Stochastic Approximations for the Macroscopic Fundamental Diagram of Urban Networks (Accepted)," *Transportation Research Part B: Methodological*, 2015.

[34] Lax, P. D., "Hyperbolic systems of conservation laws II," *Communications on Pure and Applied Mathematics*, vol. 10, no. 4, pp. 537–566, 1957.

[35] Lighthill, M. J. and Whitham, G. B., "On Kinematic Waves. II. A Theory of Traffic Flow on Long Crowded Roads," *Proceedings of the Royal Society A: Mathematical, Physical and Engineering Sciences*, vol. 229, pp. 317–345, May 1955.

[36] Mazloumian, A., Geroliminis, N., and Helbing, D., "The spatial variability of vehicle densities as determinant of urban network capacity.," *Philosophical transactions. Series A, Mathematical, physical, and engineering sciences*, vol. 368, pp. 4627–47, Oct. 2010.

[37] Meyer, M. D. and Miller, E. J., *Urban Transportation Planning*. McGraw-Hill, 2nd ed., 2001.

[38] Munoz, J. and Daganzo, C. F., "Moving bottlenecks: a theory grounded on experimental observation," *Transportation and Traffic Theory in the 21st*, 2002.

[39] Nagel, K. and Schreckenberg, M., "A cellular automaton model for freeway traffic," *Journal de physique. I*, vol. 2, no. 12, pp. 2221–2229, 1992.

[40] Nagel, K., Wolf, D., Wagner, P., Simon, P., and Schreckenberg, M., "Two-lane traffic rules for cellular automata: A systematic approach," *Physical Review E*, vol. 58, pp. 1425–1437, Aug. 1998.

[41] Newell, G., "A moving bottleneck," *Transportation Research Part B: Methodological*, vol. 32, pp. 531–537, Nov. 1998.

[42] Ngan, V., Sayed, T., and Abdelfatah, A., "Impacts of Various Parameters on Transit Signal Priority Effectiveness," *Journal of Public Transportation*, vol. 7, no. 3, pp. 71–93, 2004.

[43] Ran, B., Jin, P. J., Boyce, D., Qiu, T. Z., and Cheng, Y., "Perspectives on Future Transportation Research: Impact of Intelligent Transportation System Technologies on Next-Generation Transportation Modeling," *Journal of Intelligent Transportation Systems*, vol. 16, no. 4, pp. 226–242, 2012.

[44] Richards, P. I., "Shock Waves on the Highway," *Operations Research*, vol. 4, pp. 42–51, Feb. 1956.

[45] Ross, S., *Introduction to Probability Models*. Academic Press, 10th ed., 2010.

[46] Sbayti, H. and Roden, D., "Best Practices in the Use of Micro Simulation," *American Association of State Highway and Transportation Officials*, no. March, pp. 1–76, 2010.

[47] Tupper, L. L., Chowdhury, M. a., Klotz, L., and Fries, R. N., "Measuring Sustainability: How Traffic Incident Management through Intelligent Transportation Systems has Greater Energy and Environmental Benefits than Common Construction-Phase Strategies for Green Roadways," *International Journal of Sustainable Transportation*, vol. 6, no. 5, pp. 282–297, 2012.

[48] Watkins, K. E., Ferris, B., Borning, A., Rutherford, G. S., and Layton, D., "Where Is My Bus? Impact of mobile real-time information on the perceived and actual wait time of transit riders," *Transportation Research Part A: Policy and Practice*, vol. 45, pp. 839–848, Oct. 2011.

[49] Xie, X., Chiabaut, N., and Leclercq, L., "Macroscopic Fundamental Diagram for Urban Streets and Mixed Traffic," *Transportation Research Record: Journal of the Transportation Research Board*, vol. 2390, pp. 1–10, Dec. 2013.

[50] Zhao, X. M., Gao, Z. Y., and Jia, B., "The capacity drop caused by the combined effect of the intersection and the bus stop in a CA model," *Physica A: Statistical Mechanics and its Applications*, vol. 385, no. 2, pp. 645–658, 2007.

[51] Zhao, X. M., Gao, Z. Y., and Li, K. P., "The capacity of two neighbour intersections considering the influence of the bus stop," *Physica A: Statistical Mechanics and its Applications*, vol. 387, no. 18, pp. 4649–4656, 2008.

[52] Zhao, Y. and Kockelman, K. M., "The propagation of uncertainty through travel demand models: An exploratory analysis," *The Annals of Regional Science*, vol. 36, pp. 145–163, Feb. 2002.

[53] Zheng, N. and Geroliminis, N., "On the distribution of urban road space for multimodal congested networks," *Transportation Research Part B: Methodological*, vol. 57, pp. 326–341, Nov. 2013.

[54] Zhu, H., "Numerical study of urban traffic flow with dedicated bus lane and intermittent bus lane," *Physica A: Statistical Mechanics and its Applications*, vol. 389, pp. 3134–3139, Aug. 2010.